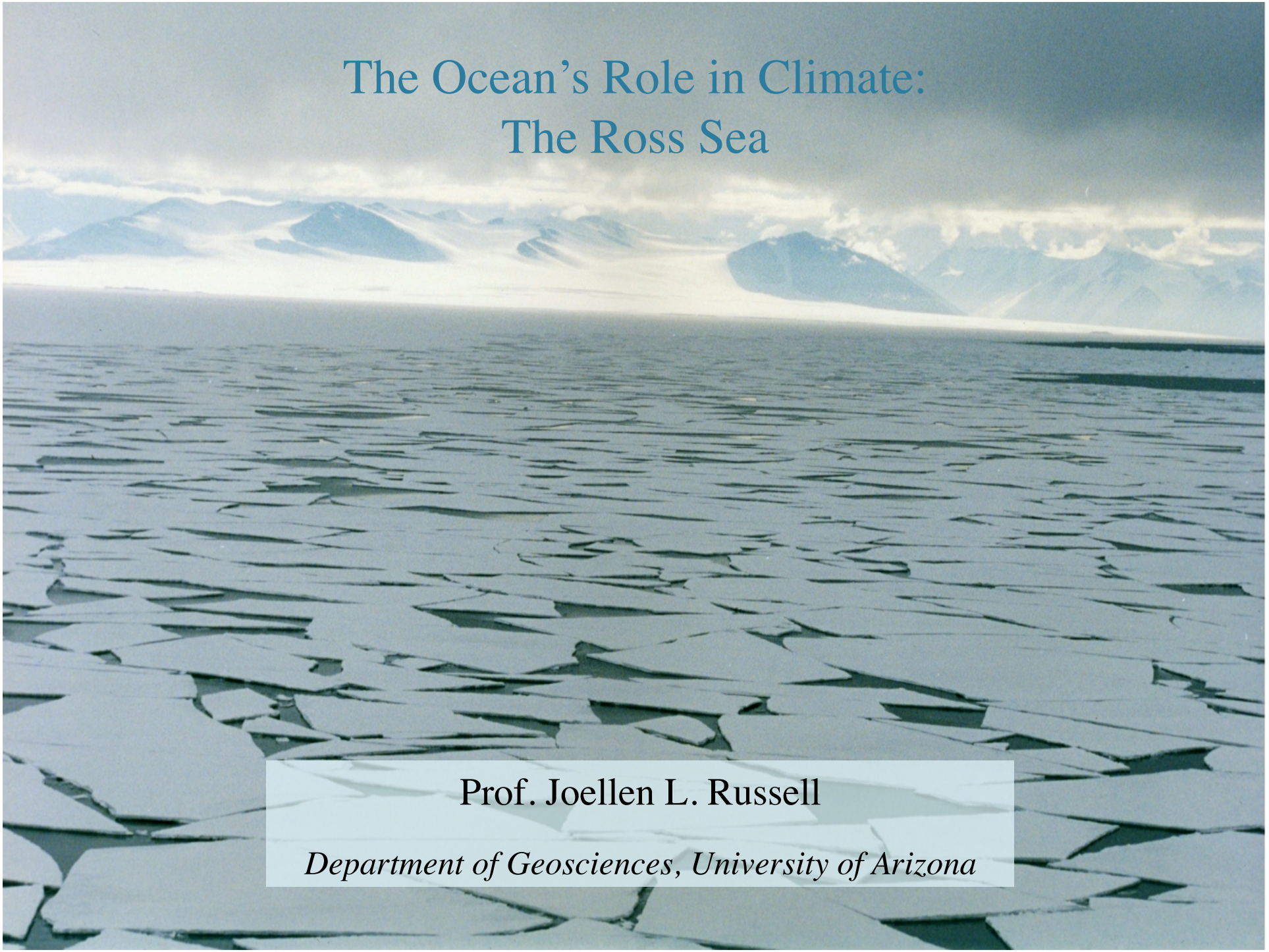

The Ocean's Role in Climate: The Ross Sea

Prof. Joellen L. Russell

Department of Geosciences, University of Arizona

Collaborators

Tom Delworth, Keith Dixon, Ron Stouffer, John Dunne & Robbie Toggweiler

Geophysical Fluid Dynamics Laboratory - NOAA

Challenges

The carbon and heat uptake of the Southern Ocean is one of the primary sources of error in projecting climate change.

A. 85% of the anthropogenic carbon currently entering the atmosphere will dissolve in the ocean - the rate is limited by the rate at which deep waters are exposed to the surface.

B. The Southern Ocean accounts for about 40% of the total oceanic uptake of carbon and controls the air-sea gas fluxes associated with the biological pump

C. There is significant disagreement between models about the rate at which heat and carbon will be taken up by the Southern Ocean and the deep ocean globally.

Energy Content in the Climate System

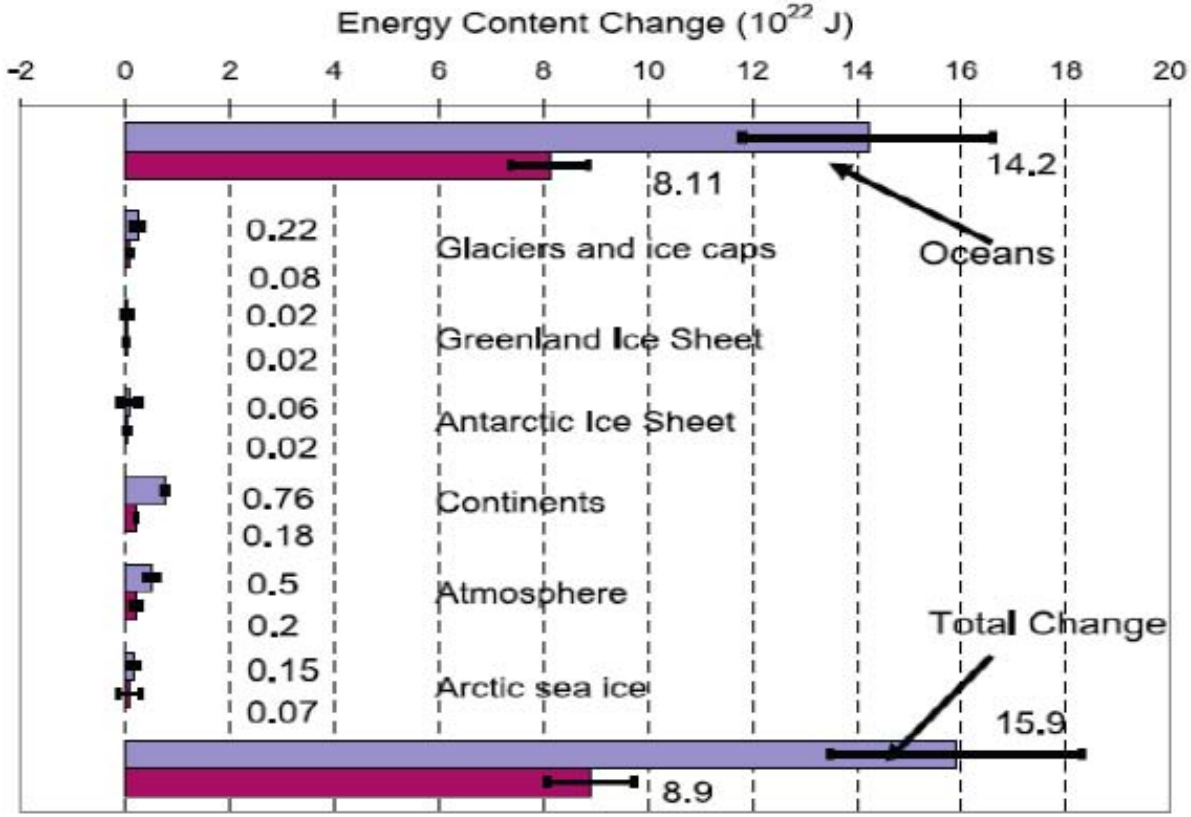

Fig. 2. Energy content changes in different components of the Earth system for two periods (1961–2003 and 1993–2003). Blue bars are for 1961 to 2003; burgundy bars are for 1993 to 2003. Positive energy content change means an increase in stored energy (i.e., heat content in oceans, latent heat from reduced ice or sea ice volumes, heat content in the continents excluding latent heat from permafrost changes, and latent and sensible heat and potential and kinetic energy in the atmosphere). All error estimates are 90% confidence intervals. No estimate of confidence is available for the continental heat gain. Some of the results have been scaled from published results for the two respective periods. From (IPCC 2007, Fig. TS.15 and Fig. 5.4).

Trenberth & Fasullo 2011

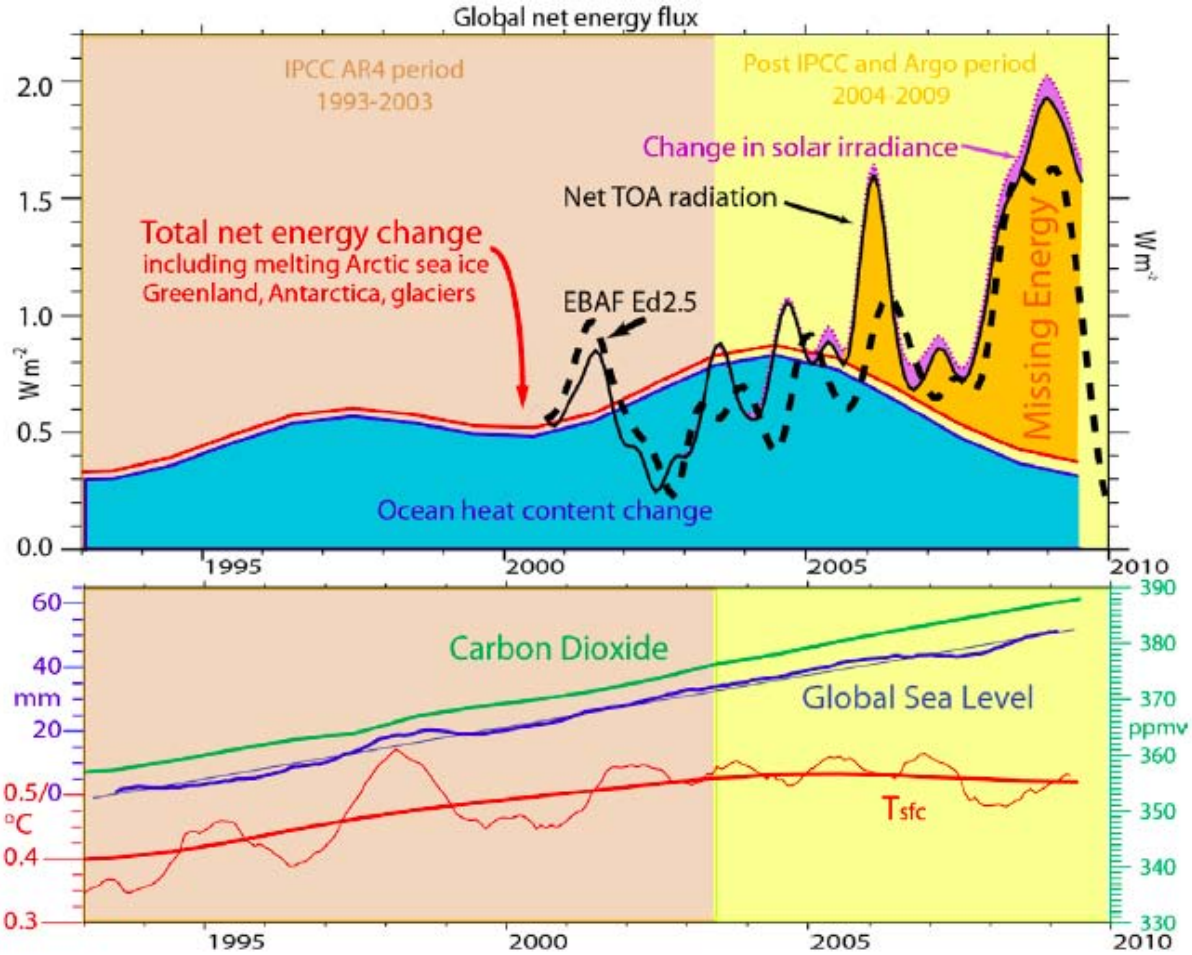

Figure 4. The disposition of energy entering the climate system is estimated. The observed changes (lower panel; Trenberth and Fasullo 2010) show the 12-month running means of global mean surface temperature anomalies relative to 1901-2000 from NOAA (red (thin) and decadal (thick)) in °C (scale lower left), carbon dioxide concentrations (green) in ppmv from NOAA (scale right), and global sea level adjusted for isostatic rebound from AVISO (blue, along with linear trend of 3.2 mm/yr) relative to 1993, scale at left in millimeters). Rates of change of global energy in W m^{-2} (top panel) are contrasted between the AR4-IPCC era 1993-2003 and the post-2003 Argo era. From 1992 to 2003 the decadal ocean heat content changes (blue) along with the contributions from melting glaciers, ice caps, Greenland, Antarctica and Arctic sea ice plus small contributions from land and atmosphere warming (red) suggest a total warming for the planet of 0.6±0.2 W m^{-2} (95% error bars). After 2000, preliminary observations from TOA (black) referenced to the 2000 values, as used in Trenberth and Fasullo (2010), show an increasing discrepancy (gold) relative to the total warming observed (red). The quiet sun changes in total

Trenberth & Fasullo 2011

Heat Trend Distributions

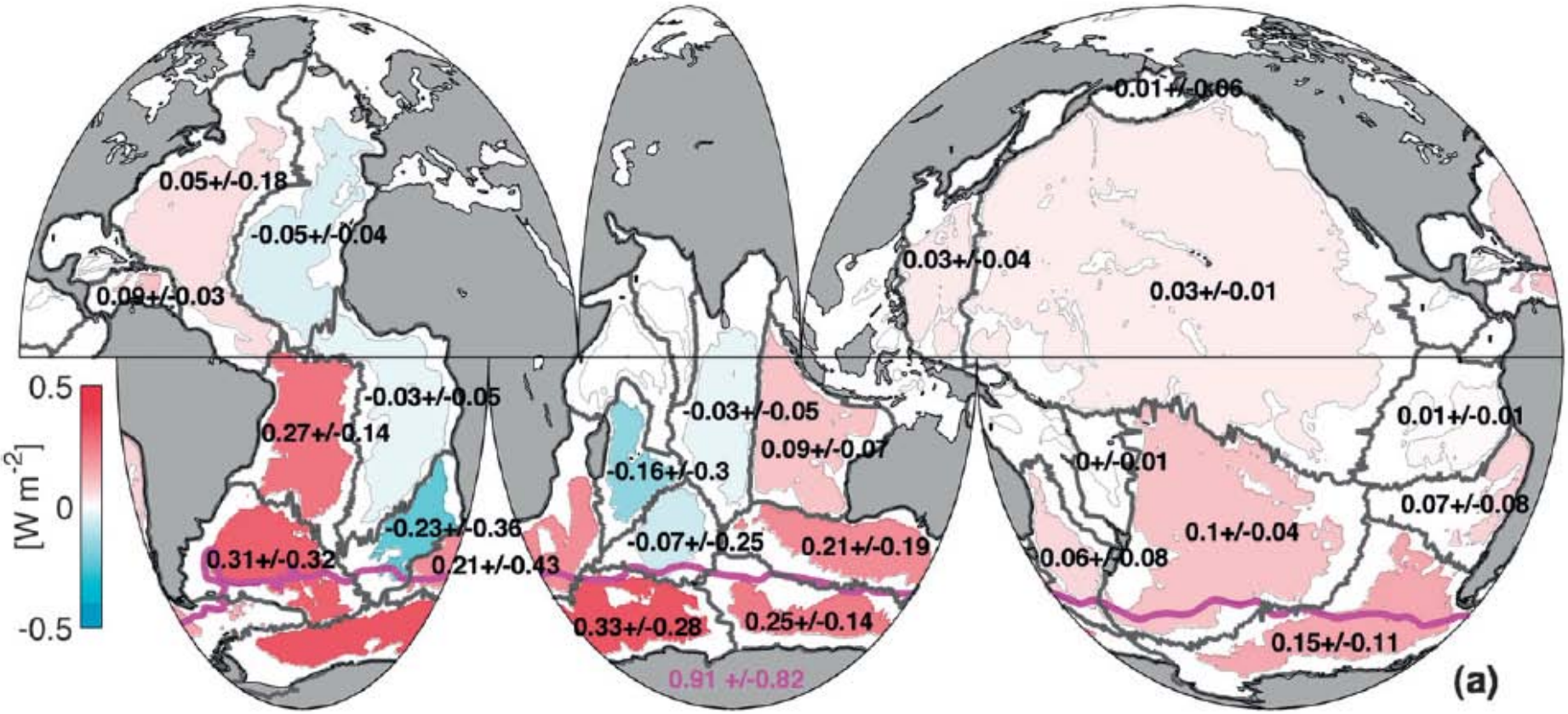

Purkey and Johnson (2010)

Southern Ocean Circulation

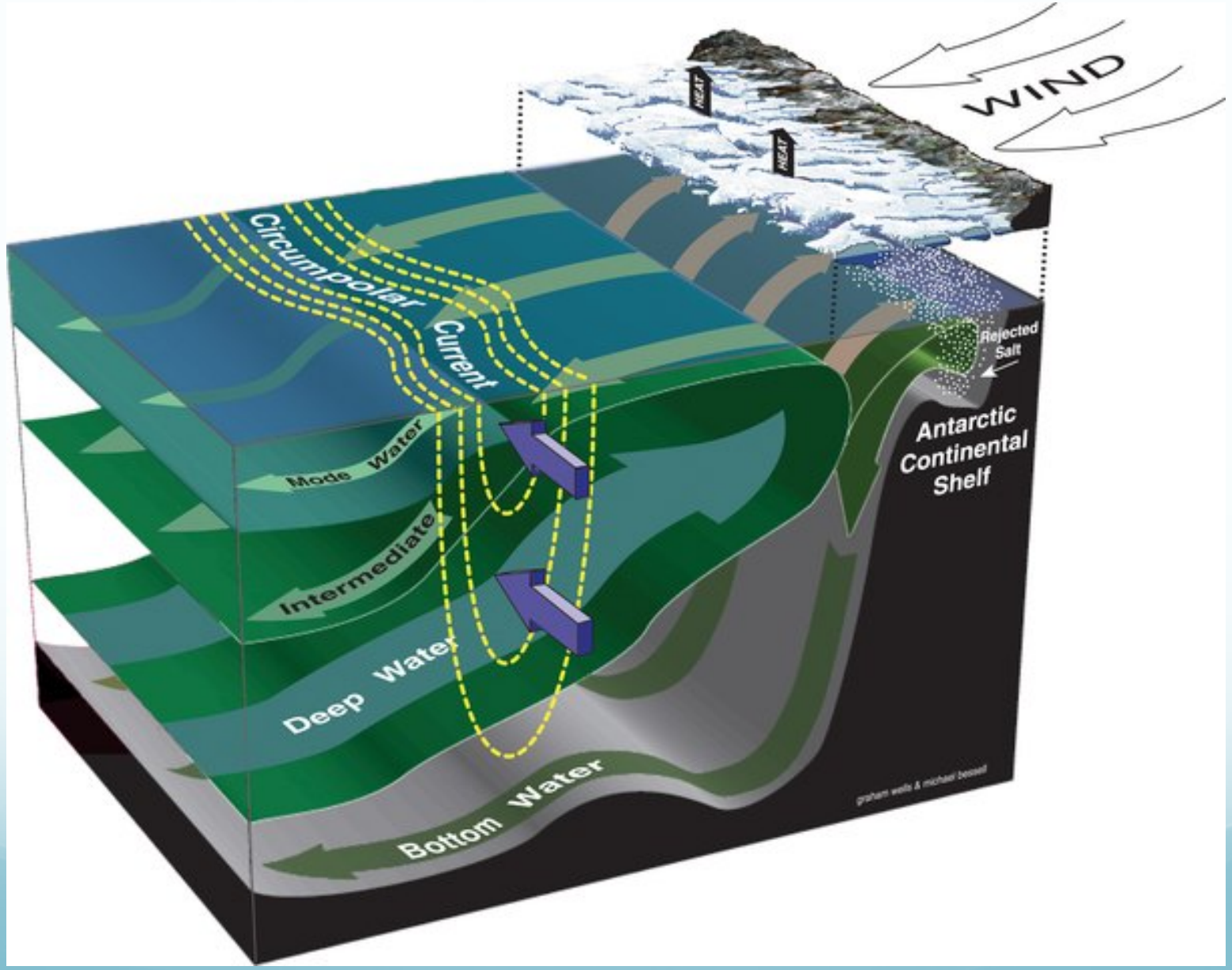

- Poleward shift of the Southern Hemisphere Westerlies

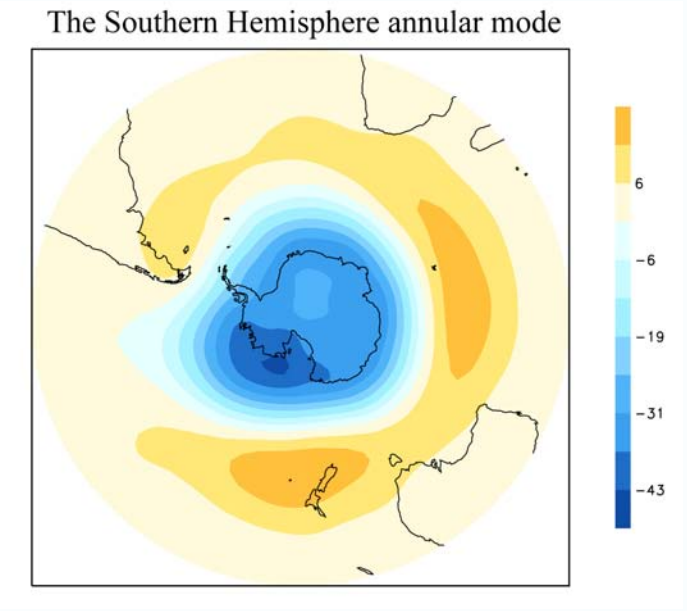

- Poleward shift of the Northern Hemisphere Westerlies

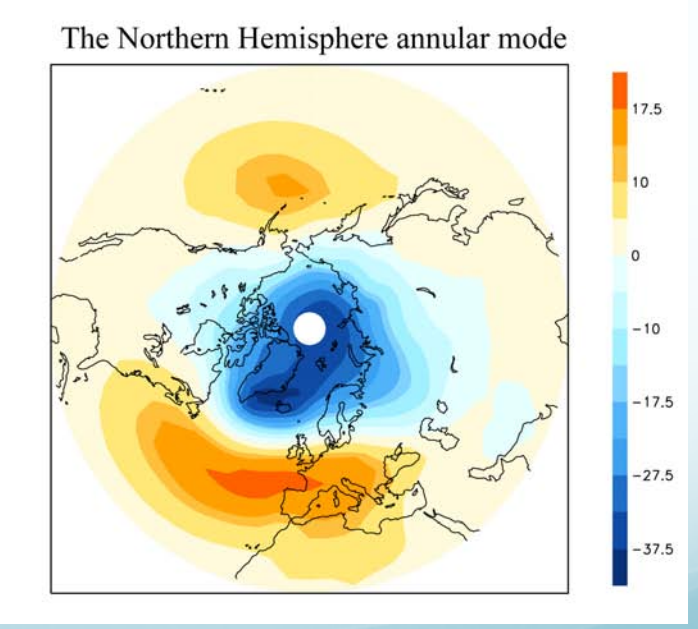

D. Thompson

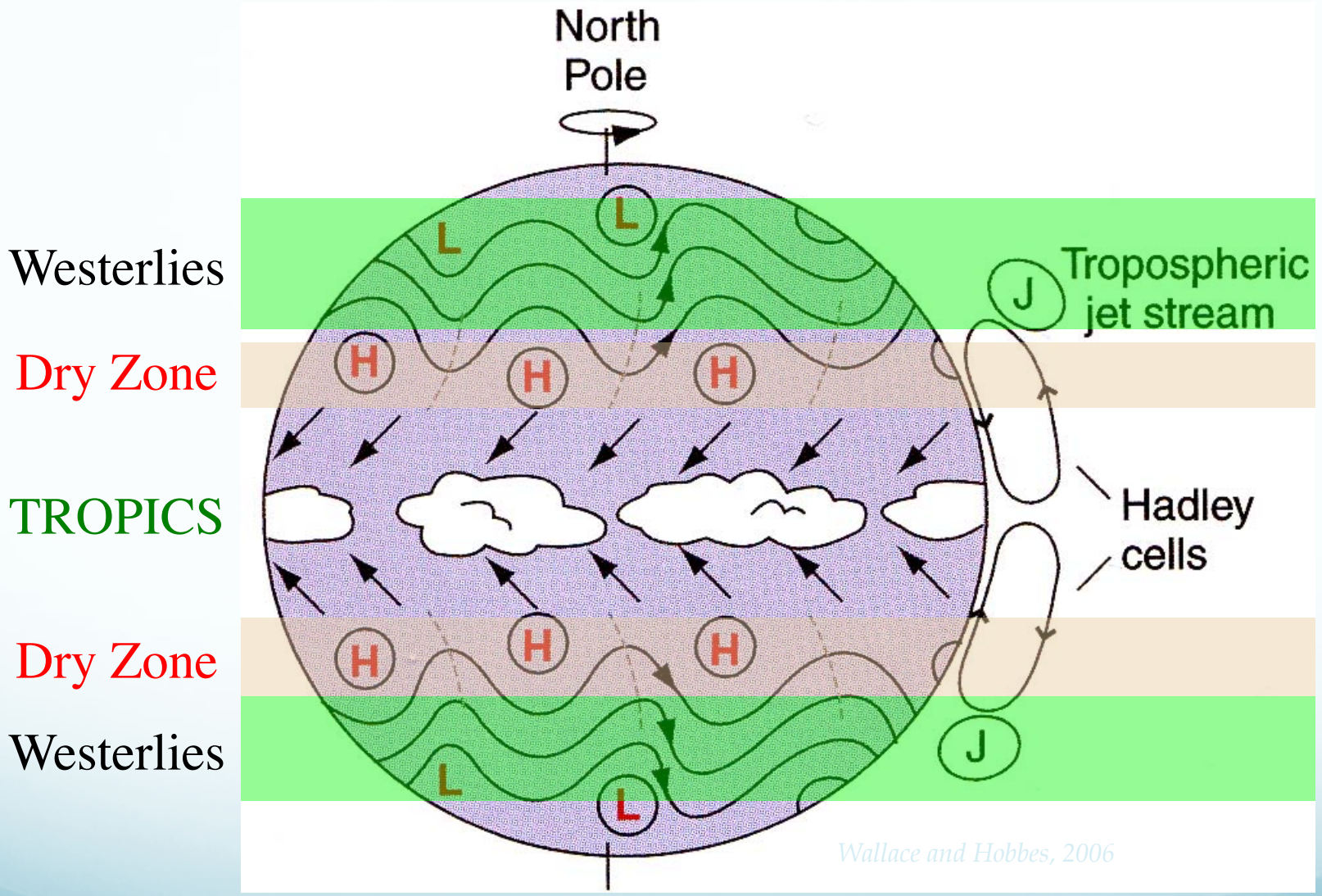
North
Pole
Westerlies
Dry Zone
TROPICS
Dry Zone
Westerlies
L
L
L
L
H
H
H
H
H
H
J
J
Tropospheric
jet stream
Hadley
cells
Wallace and Hobbes, 2006

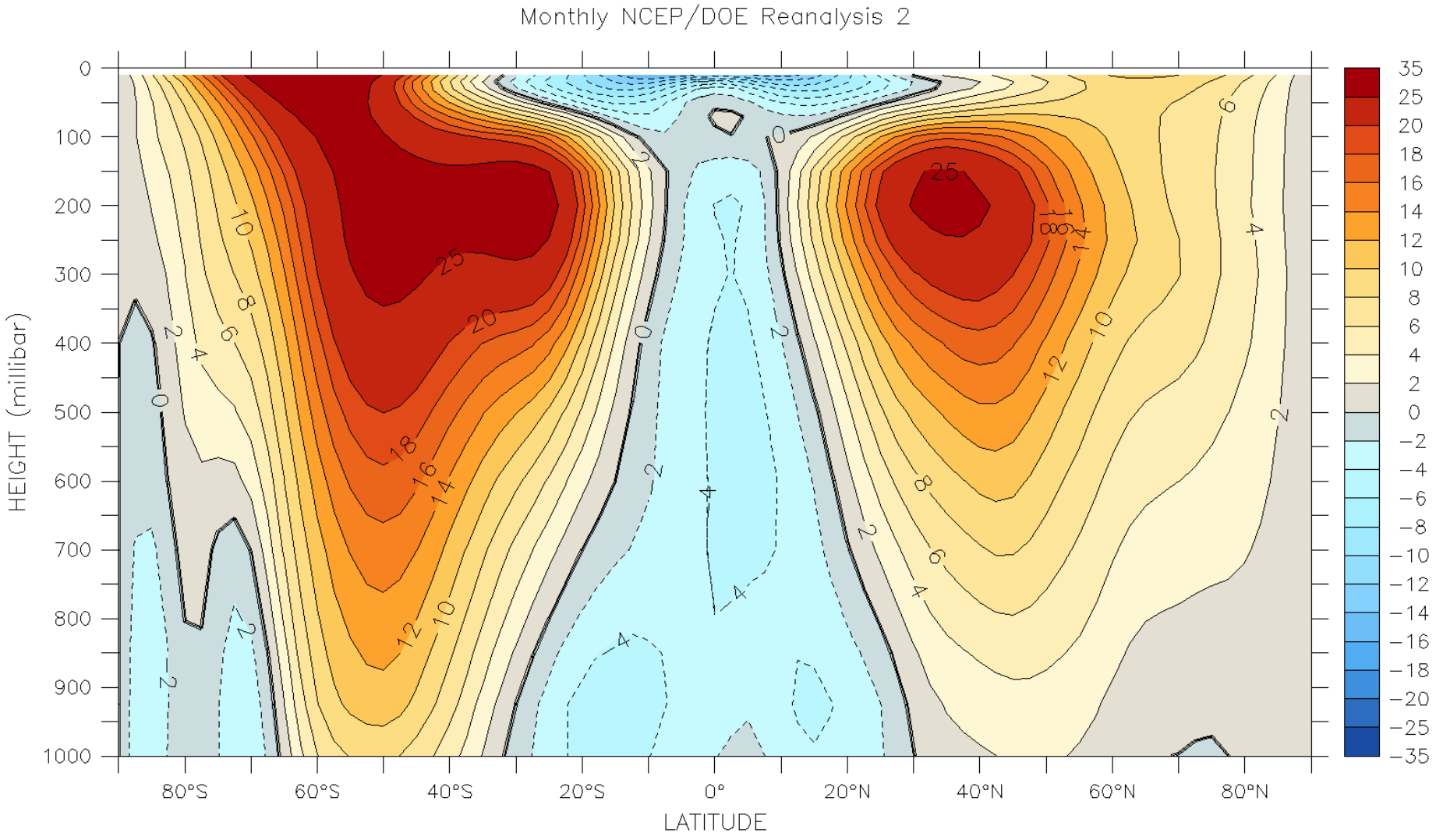

Observed Mean Zonal Wind (m/s)

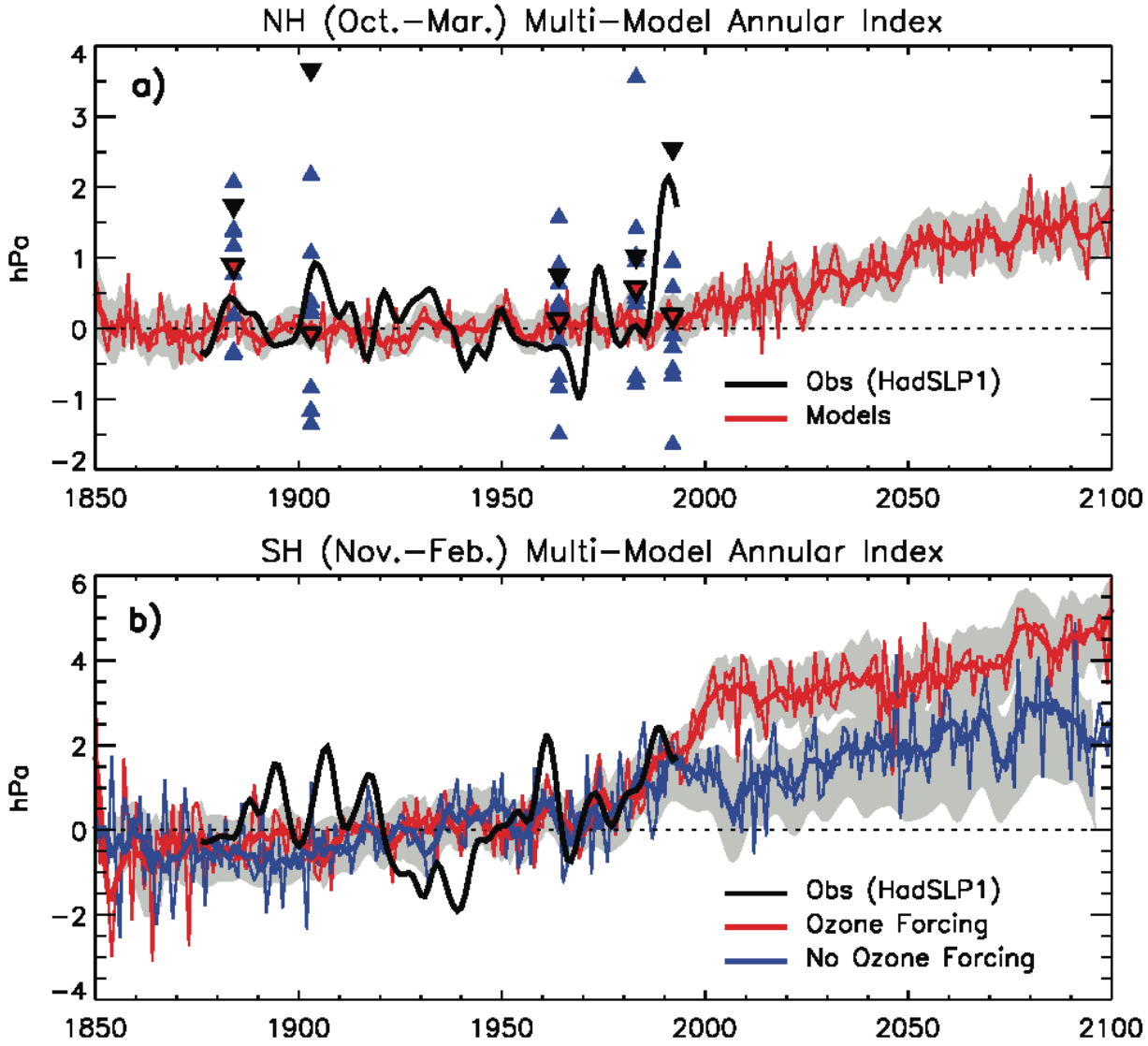

Figure 10.17. *(a) Multi-model mean of the regression of the leading EOF of ensemble mean Northern Hemisphere sea level pressure (NH SLP, thin red line). The time series of regression coefficients has zero mean between year 1900 and 1970. The thick red line is a 10-year low-pass filtered version of the mean. The grey shading represents the inter-model spread at the 95% confidence level and is filtered. A filtered version of the observed SLP from the Hadley Centre (HadSLP1) is shown in black. The regression coefficient for the winter following a major tropical eruption is marked by red, blue and black triangles for the multi-model mean, the individual model mean and observations, respectively. (b) As in (a) for Southern Hemisphere SLP for models with (red) and without (blue) ozone forcing. Adapted from Miller et al. (2006).*

Attribution of Wind Forcing (Model Results)

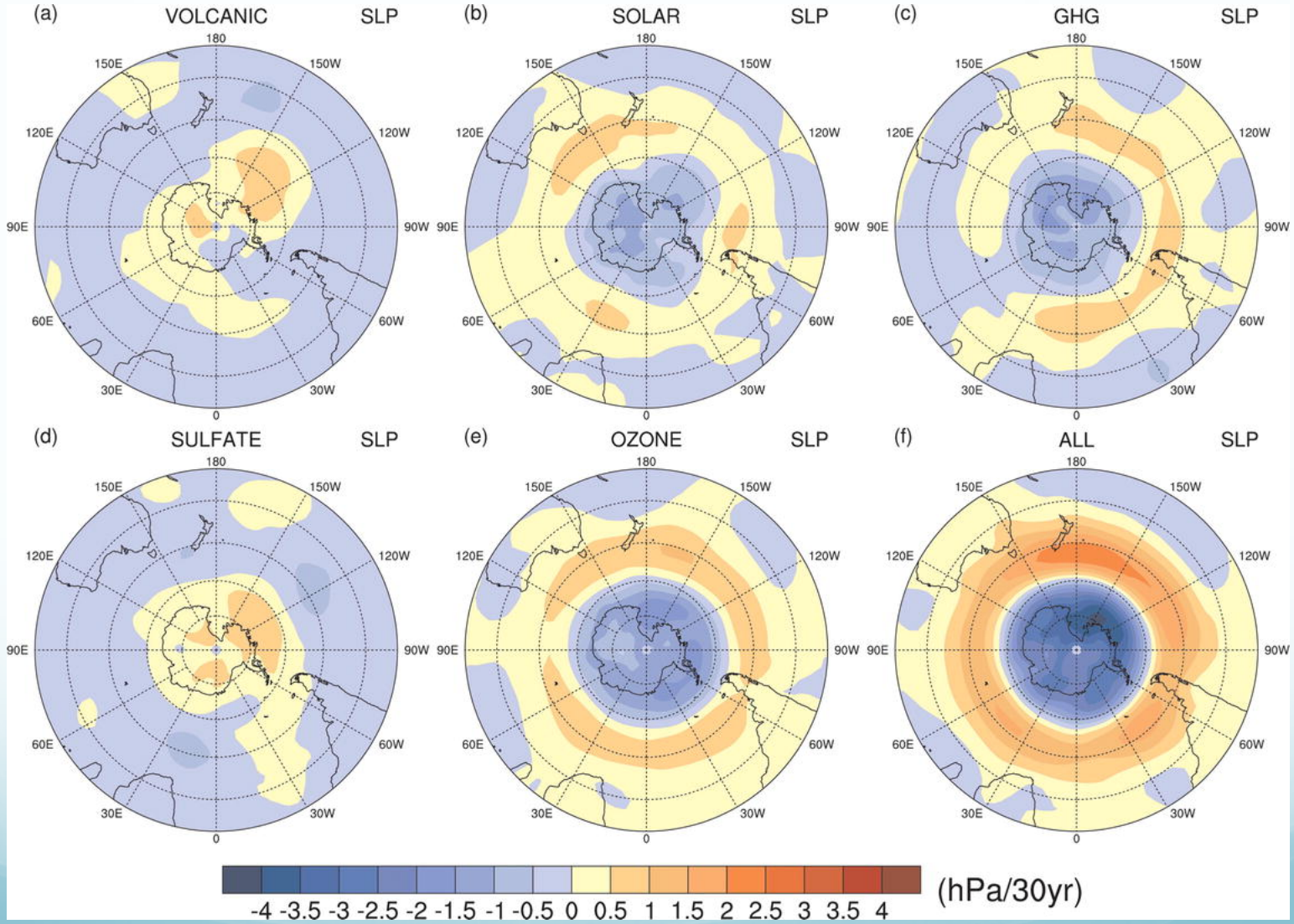

Arblaster & Meehl, 2006

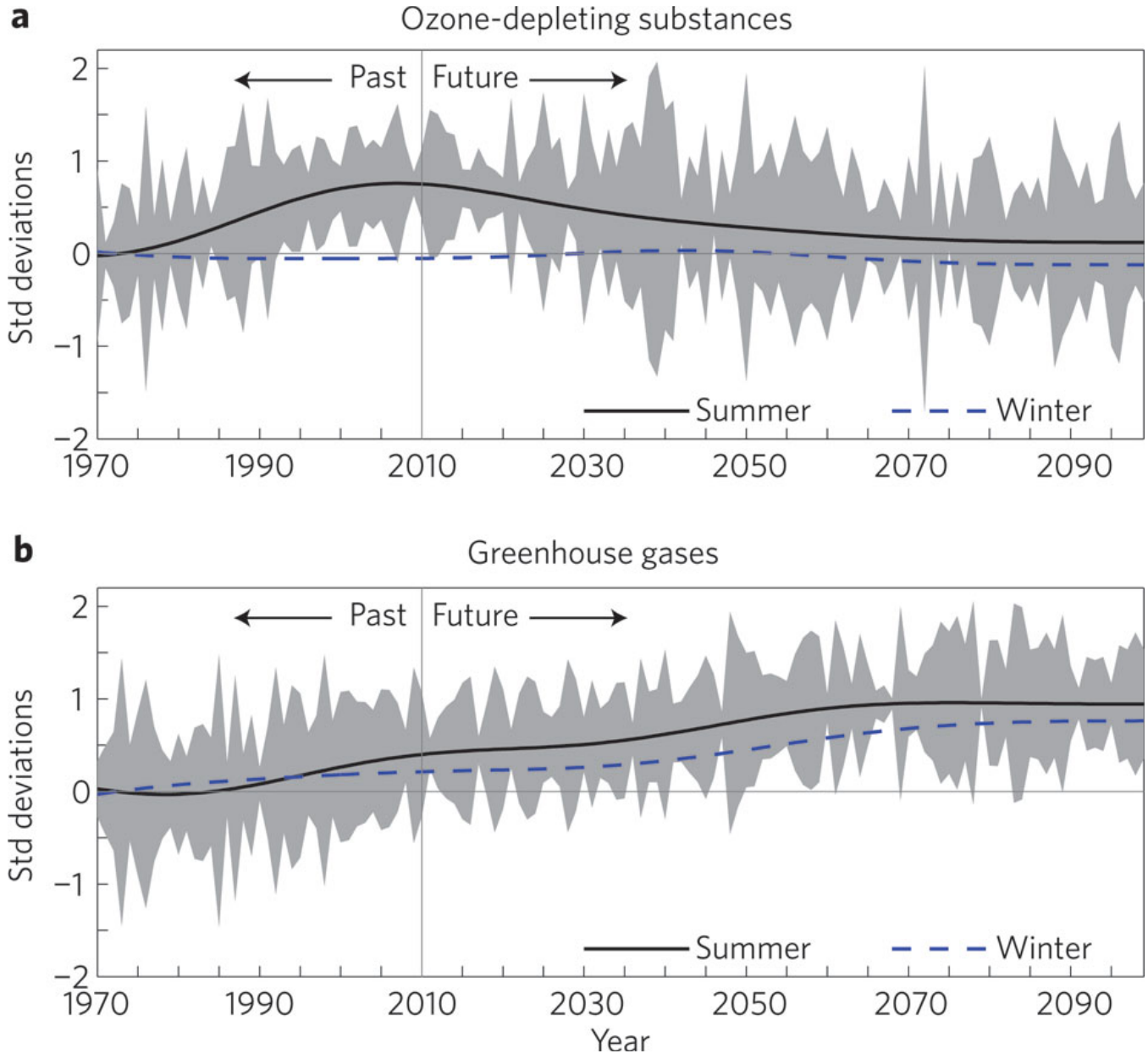

a) Forcing with ozone-depleting substances; b) forcing with greenhouse gases. (From Thompson et al., 2011)

Trajectory of Global Fossil Fuel Emissions

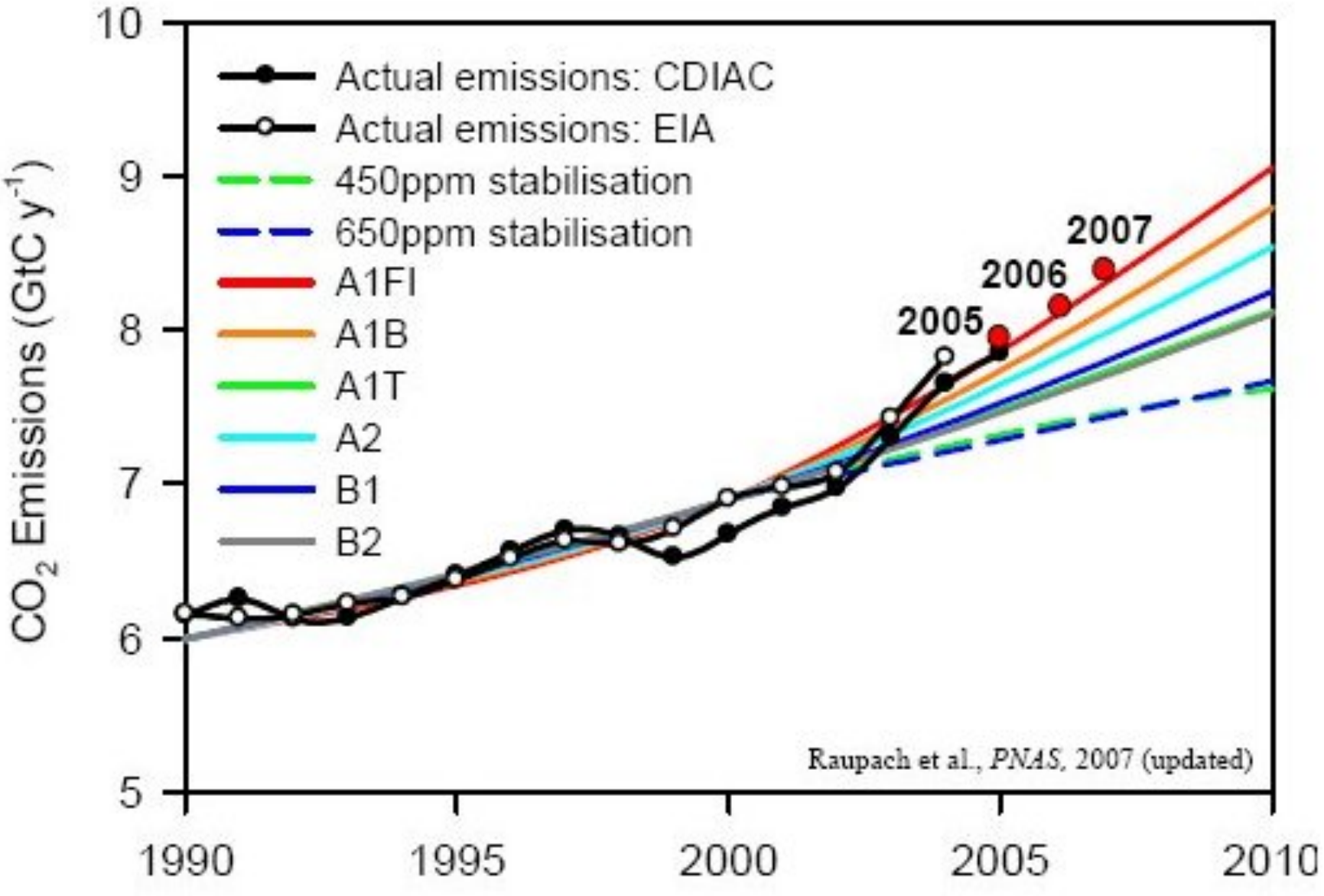

Fossil Fuel & Cement CO_2 Emissions

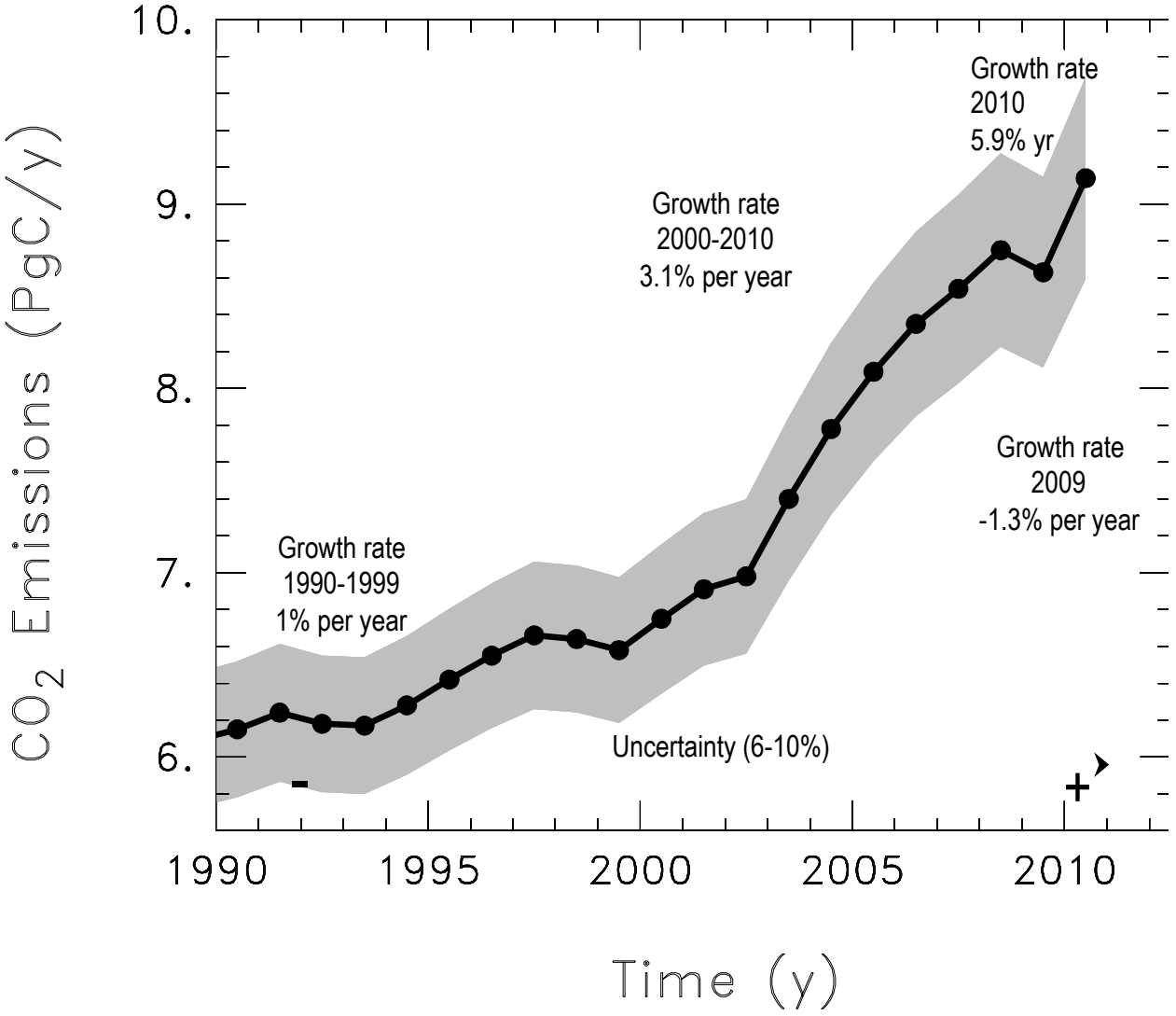

Peters et al. 2011, Nature CC; Data: Boden, Marland, Andres-CDIAC 2011; Marland et al. 2009

Atmospheric History of CFCs

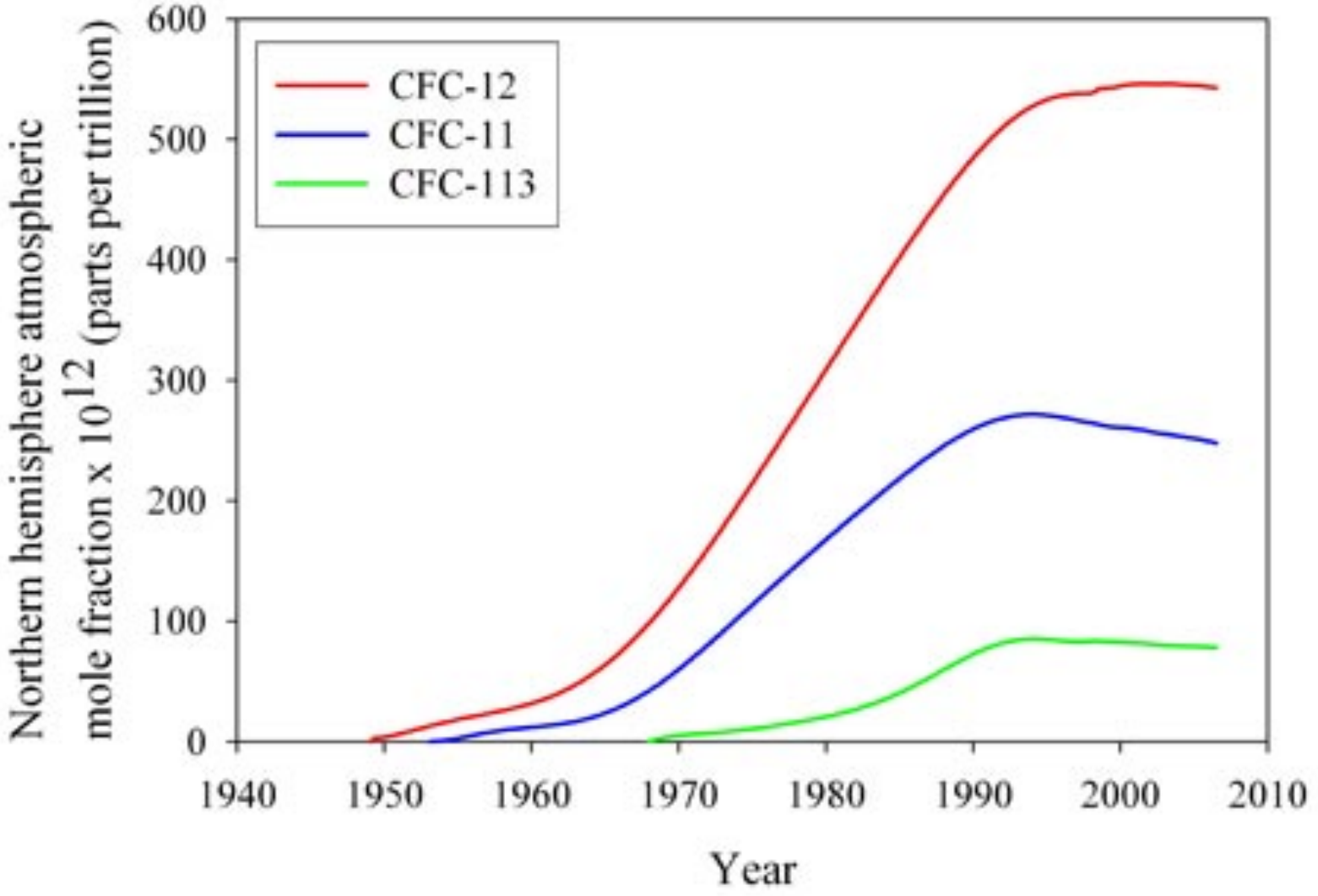

The Southern Hemisphere Ozone Hole

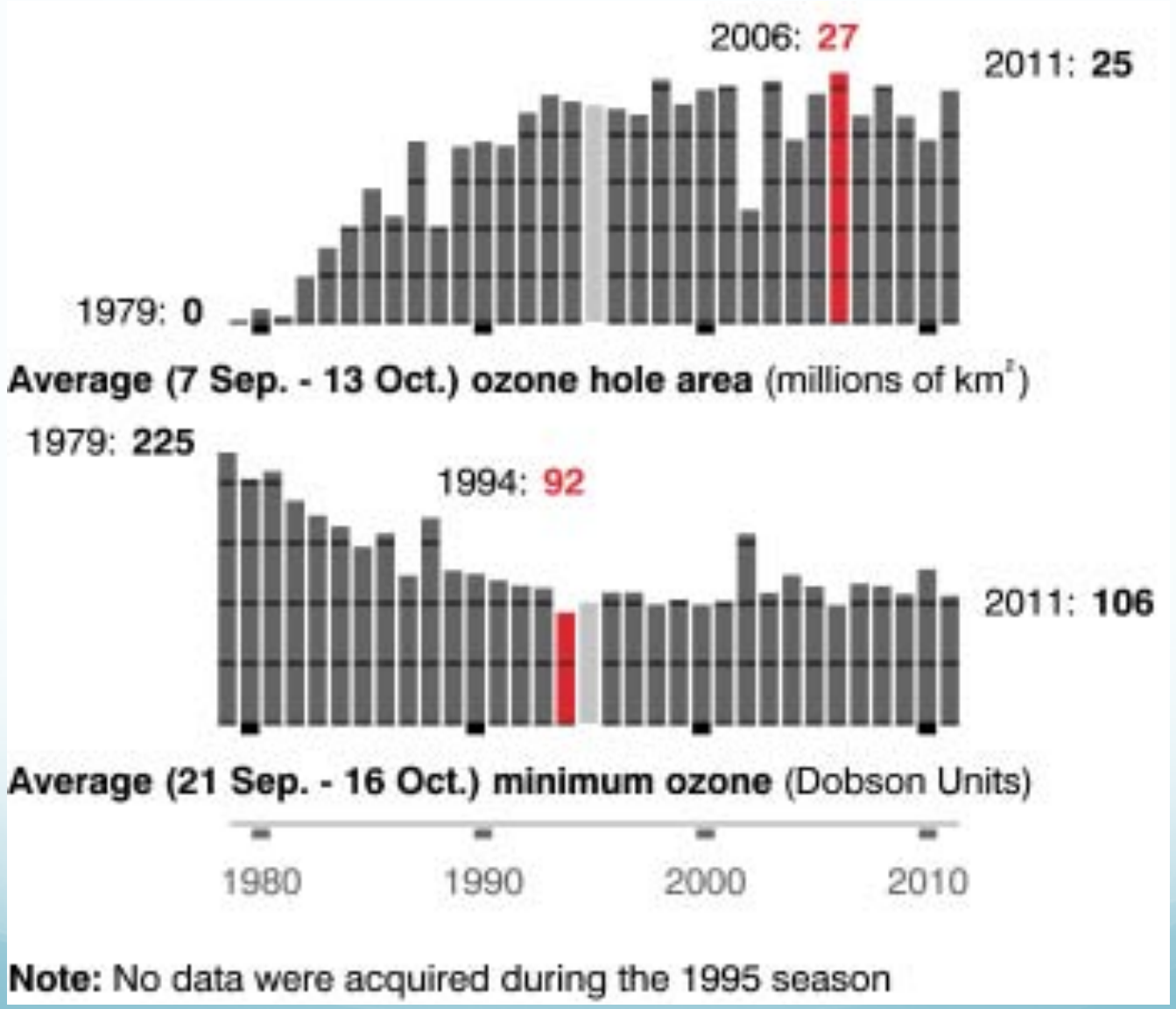

Stratospheric Temperature Trends

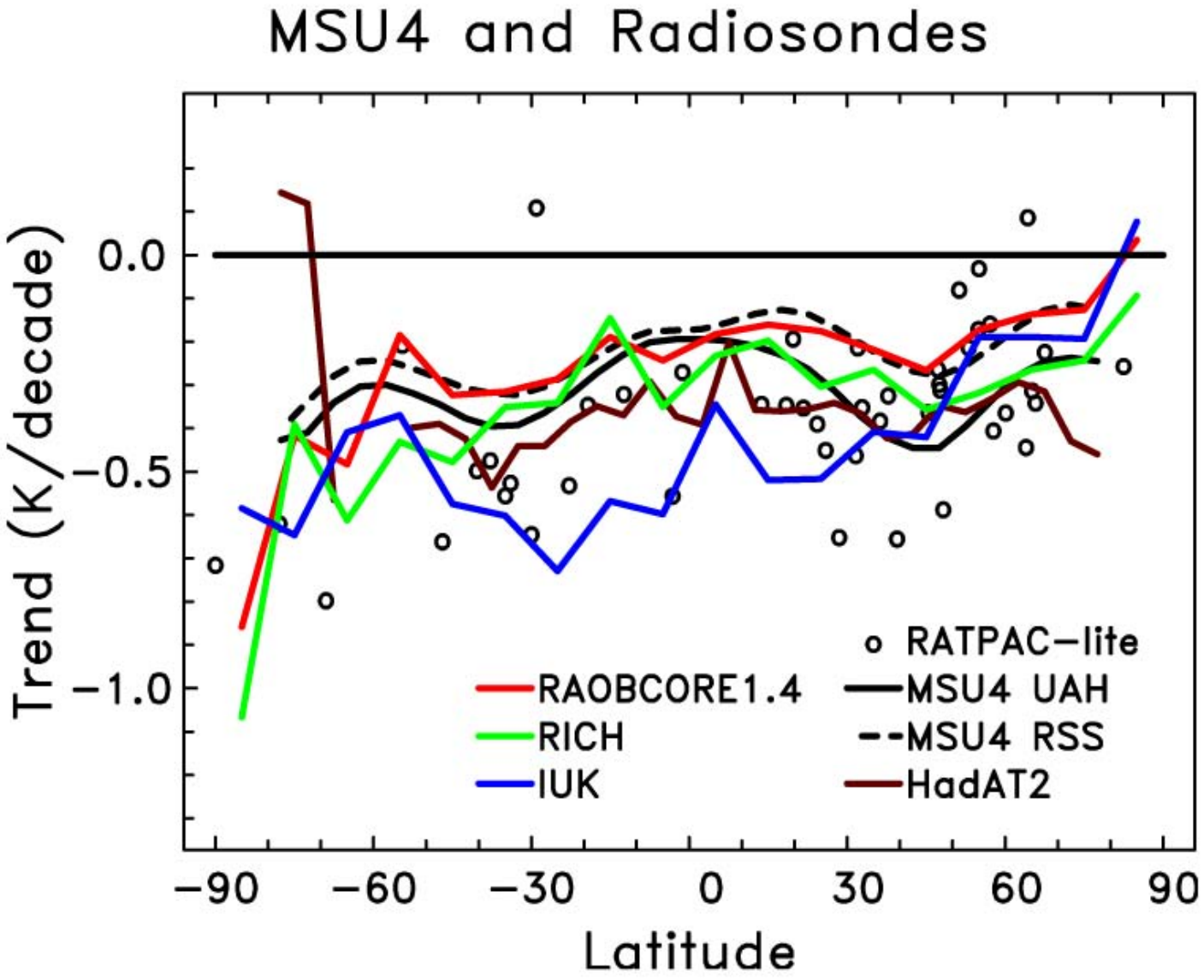

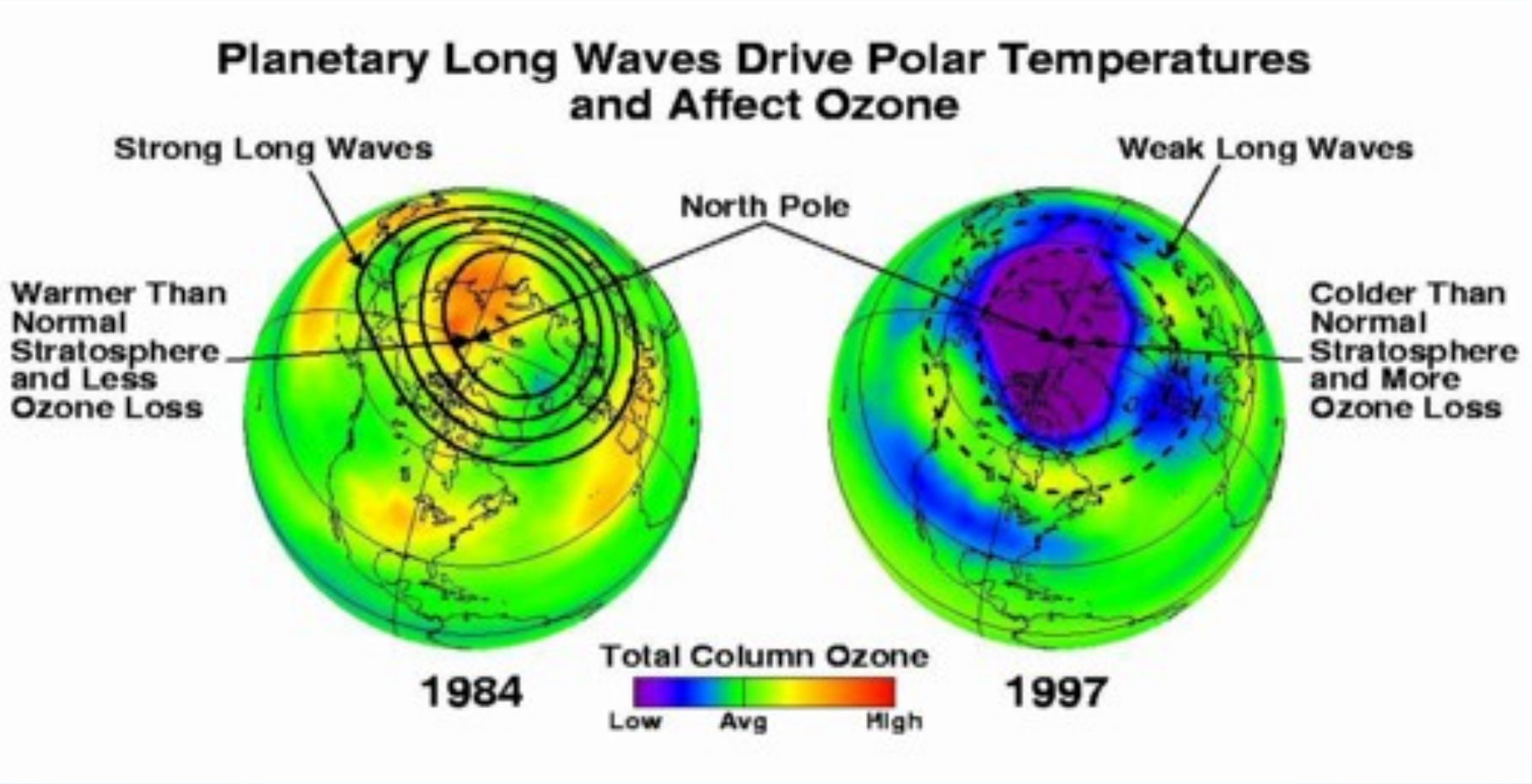

Stronger planetary waves in the northern hemisphere warm the Arctic stratosphere and suppress ozone destruction. Land forms in the southern hemisphere also produce planetary waves, but they tend to be weaker because there are fewer tall mountain ranges and more open ocean around Antarctica (NASA)

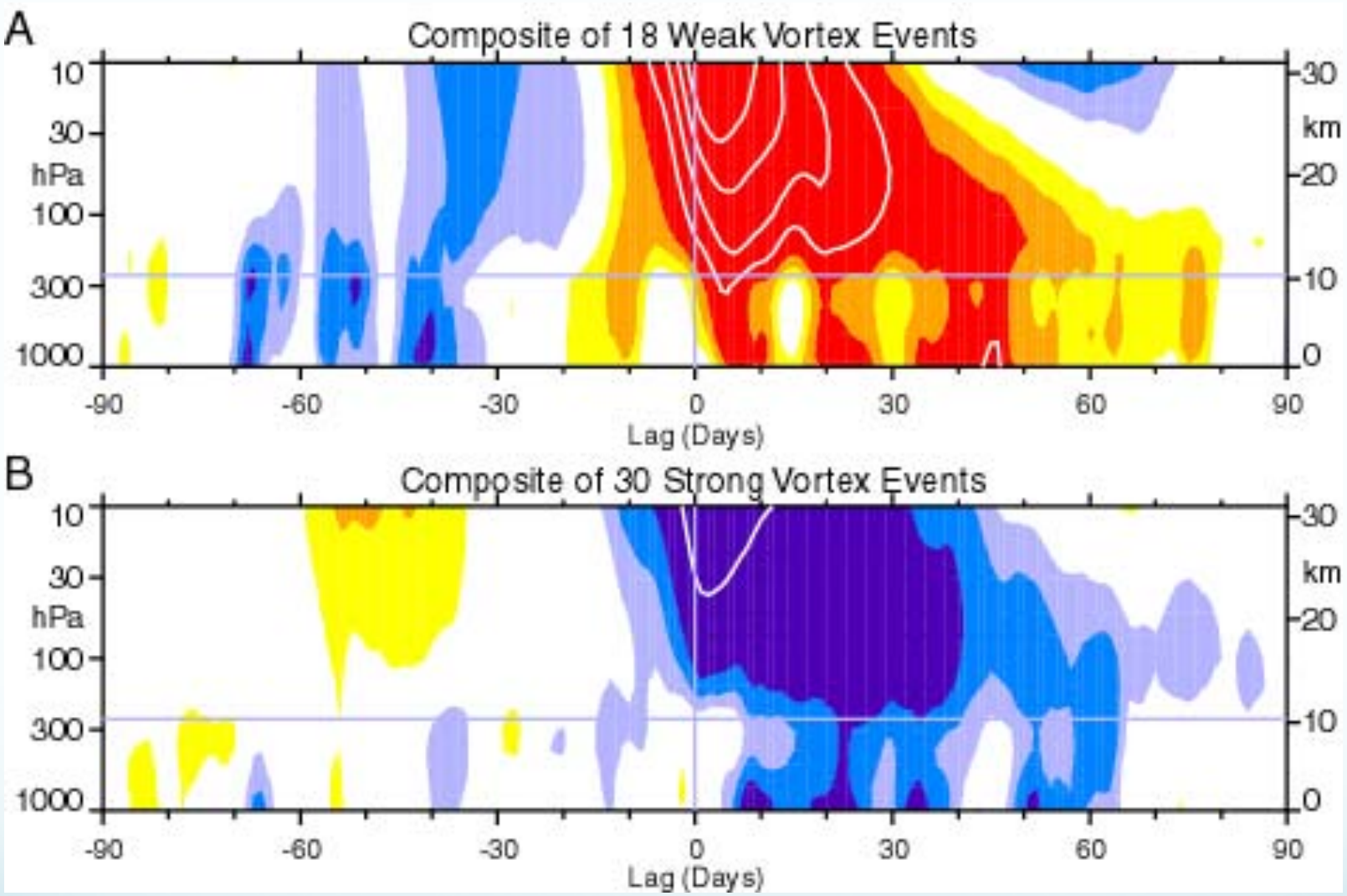

Observed composites of time-height development of the northern annular mode for (A) 18 week vortex events and (B) 30 strong vortex events.

(From: Baldwin, M. and T. J. Dunkerton (2001): Science V 294.)

Arctic Ozone Hole in Spring 2011 (NASA/JPL)

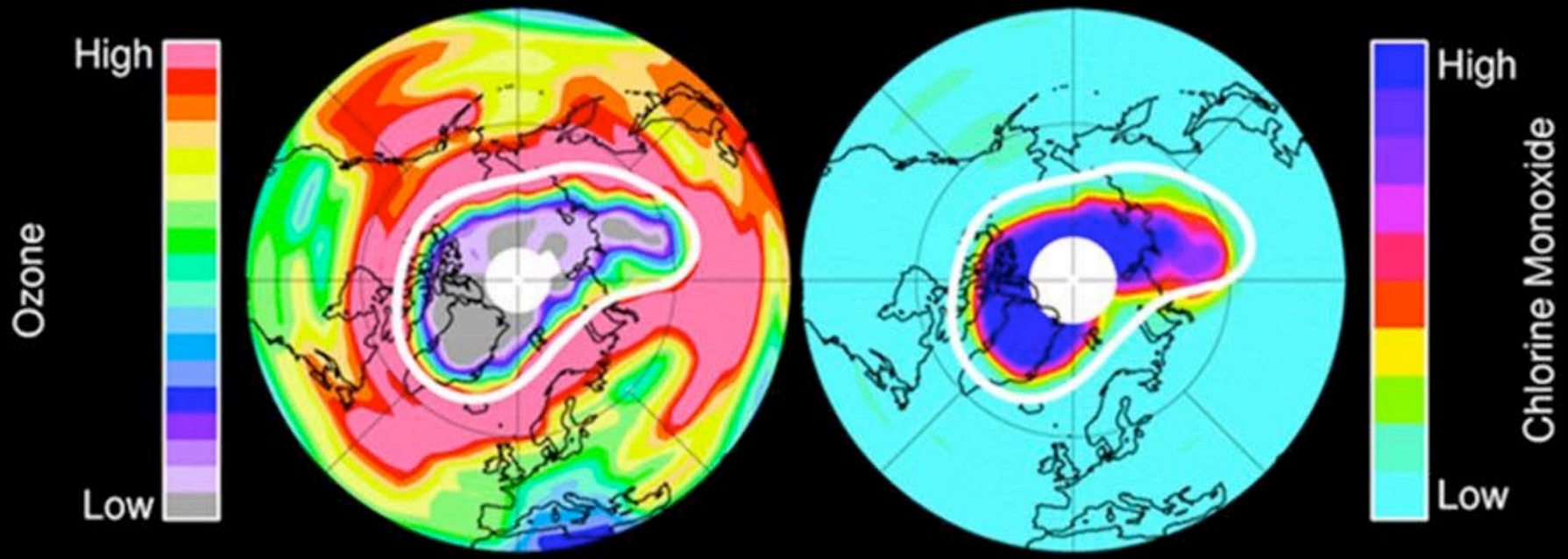

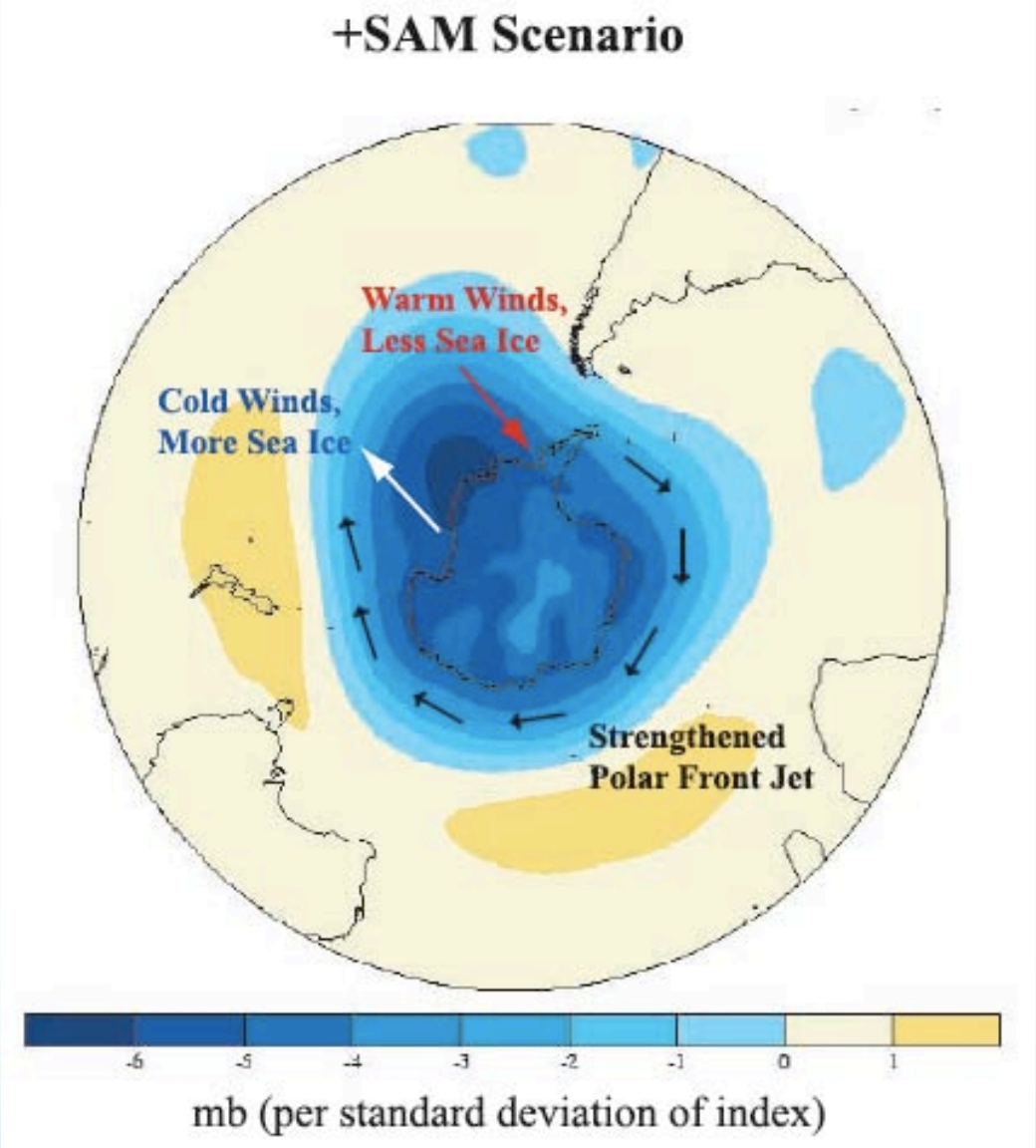

Schematic depiction of the high-latitude ice-atmosphere response to +SAM. The arrows schematically depict wind anomalies during a +SAM scenario. The base image is from T. Mitchell (http://www.jisao.washington.edu/sam) and shows the regression of SLP anomalies onto a SAM-derived index (see http://transcom.colostate.edu for details).

Stammerjohn et al. (2007)

The Ross Sea in Climate Models

Atmospheric Models

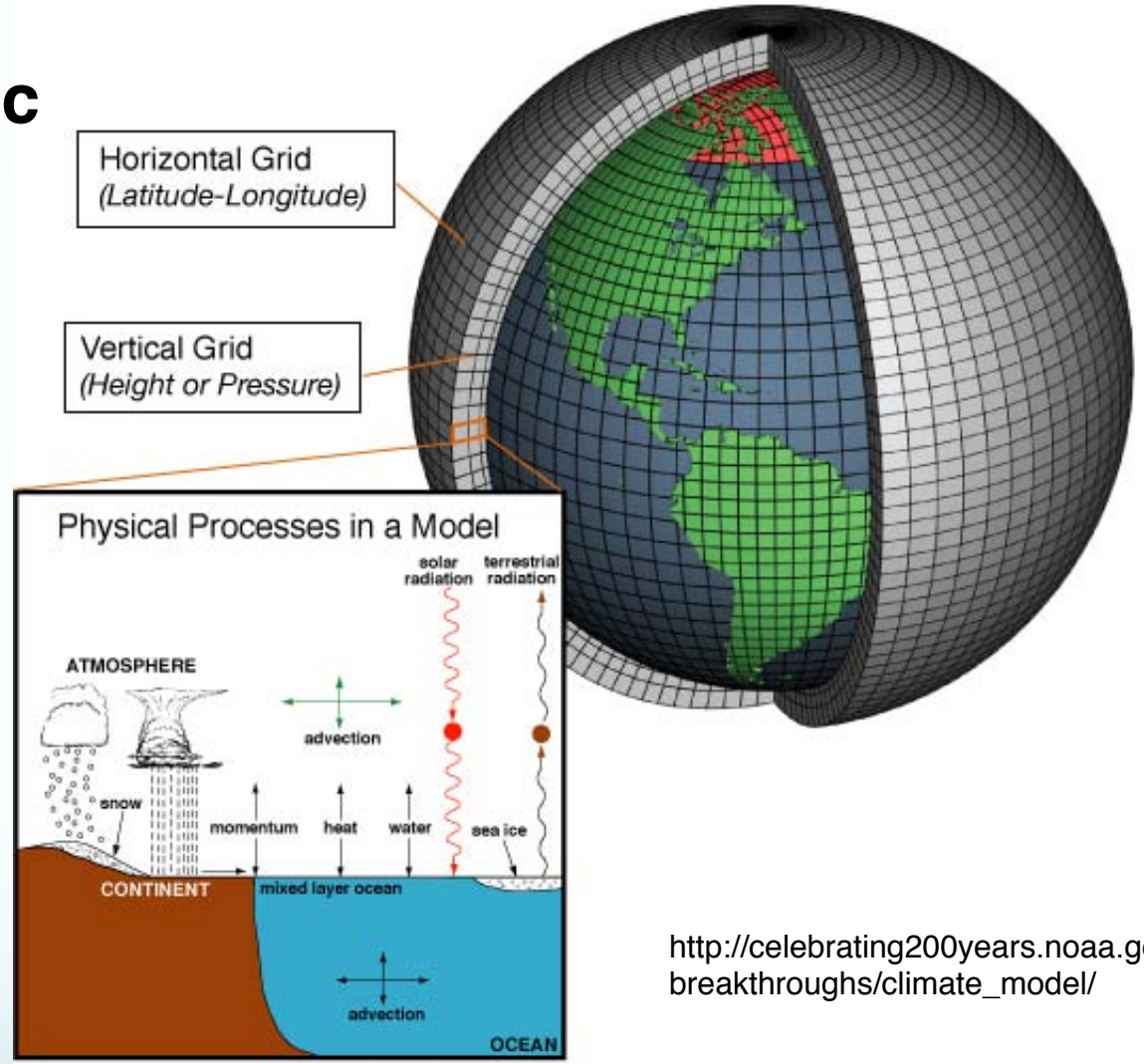

http://celebrating200years.noaa.gov/breakthroughs/climate_model/

Computer code that solves differential equations of air motion and thermodynamics to obtain time and space dependent values for temperature, wind speed, moisture and pressure in the atmosphere.

Modeling the Climate System

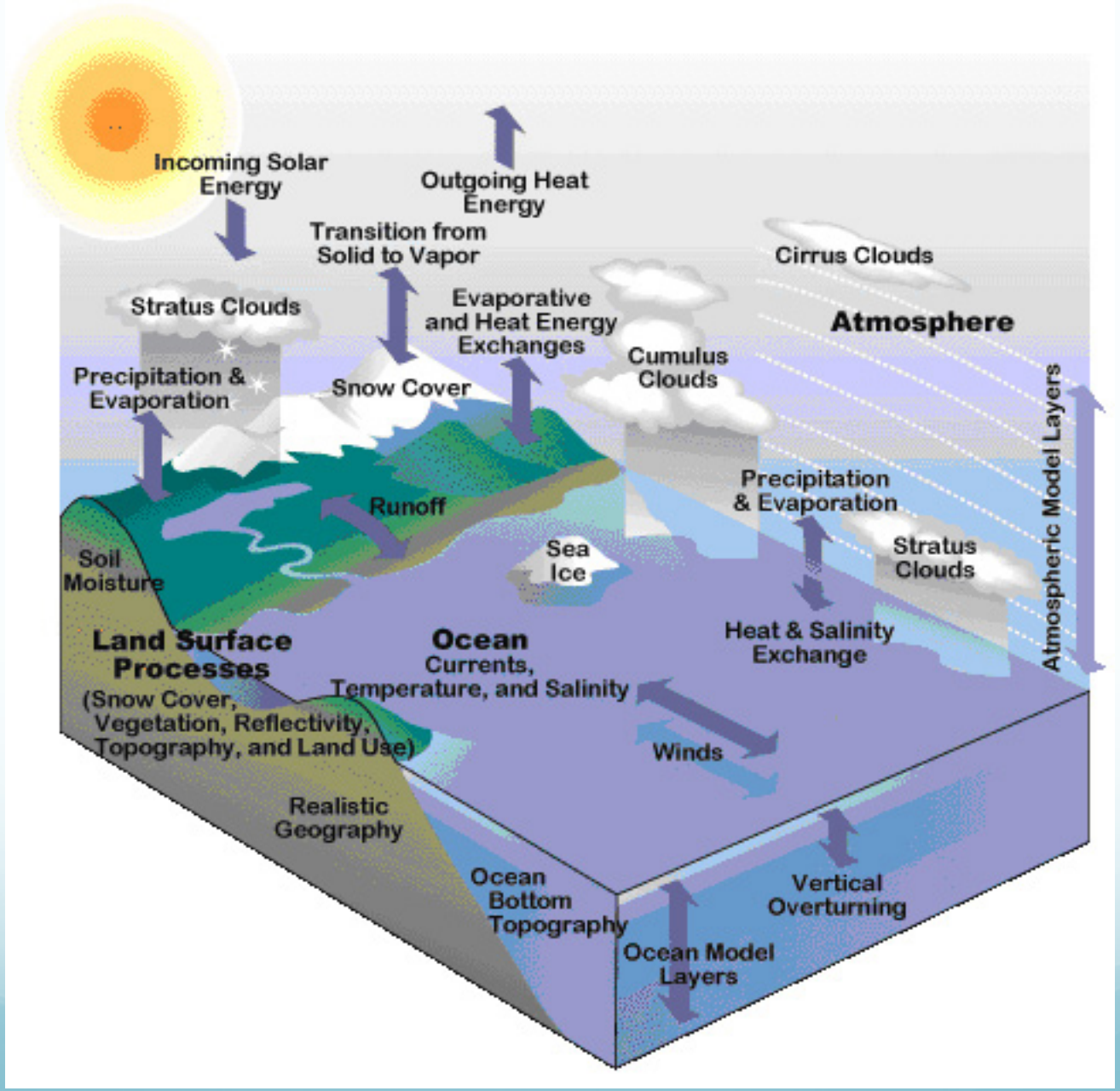

Manabe-Bryan (~1970)

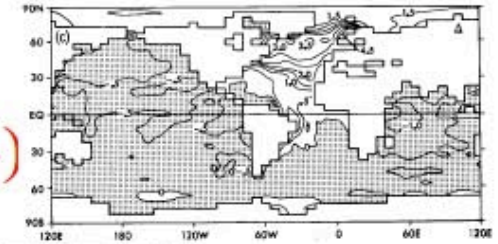

Manabe Climate Model (~1984)

CM2.0 (~2002)
CM2.1 (~2004)

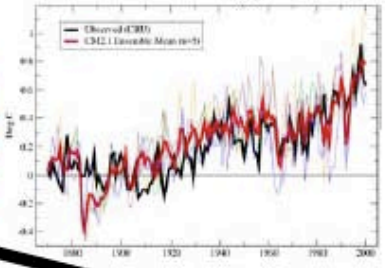

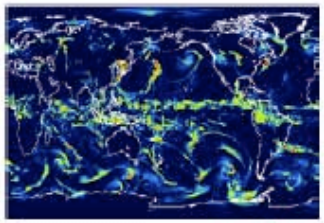

Atmos. only
(25 or 50 km Atm.)

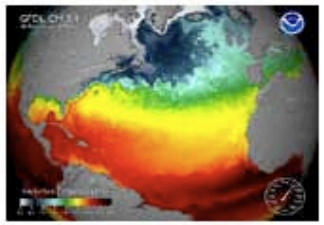

CM2.4
(1°Atm ¼° Ocn)

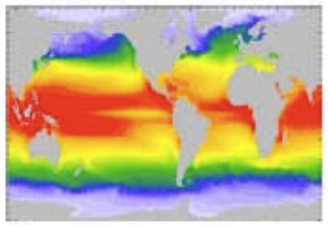

CM2M
(p* ocean)

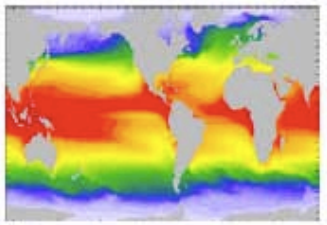

CM2G
(ρ ocean)

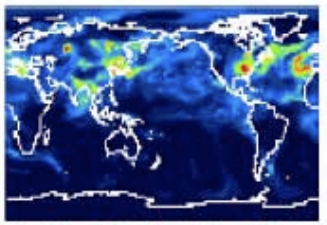

AM3/CM3x
(Atmos. chem.)

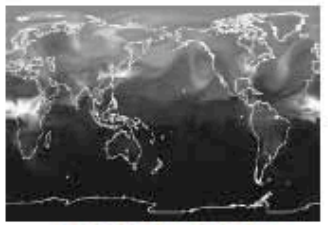

ESM2M
(Biosphere)

ESM2G
(Biosphere)

The Southern Ocean in the CMIP5 Earth System Model Simulations

An Earth System Model (ESM) closes the carbon cycle

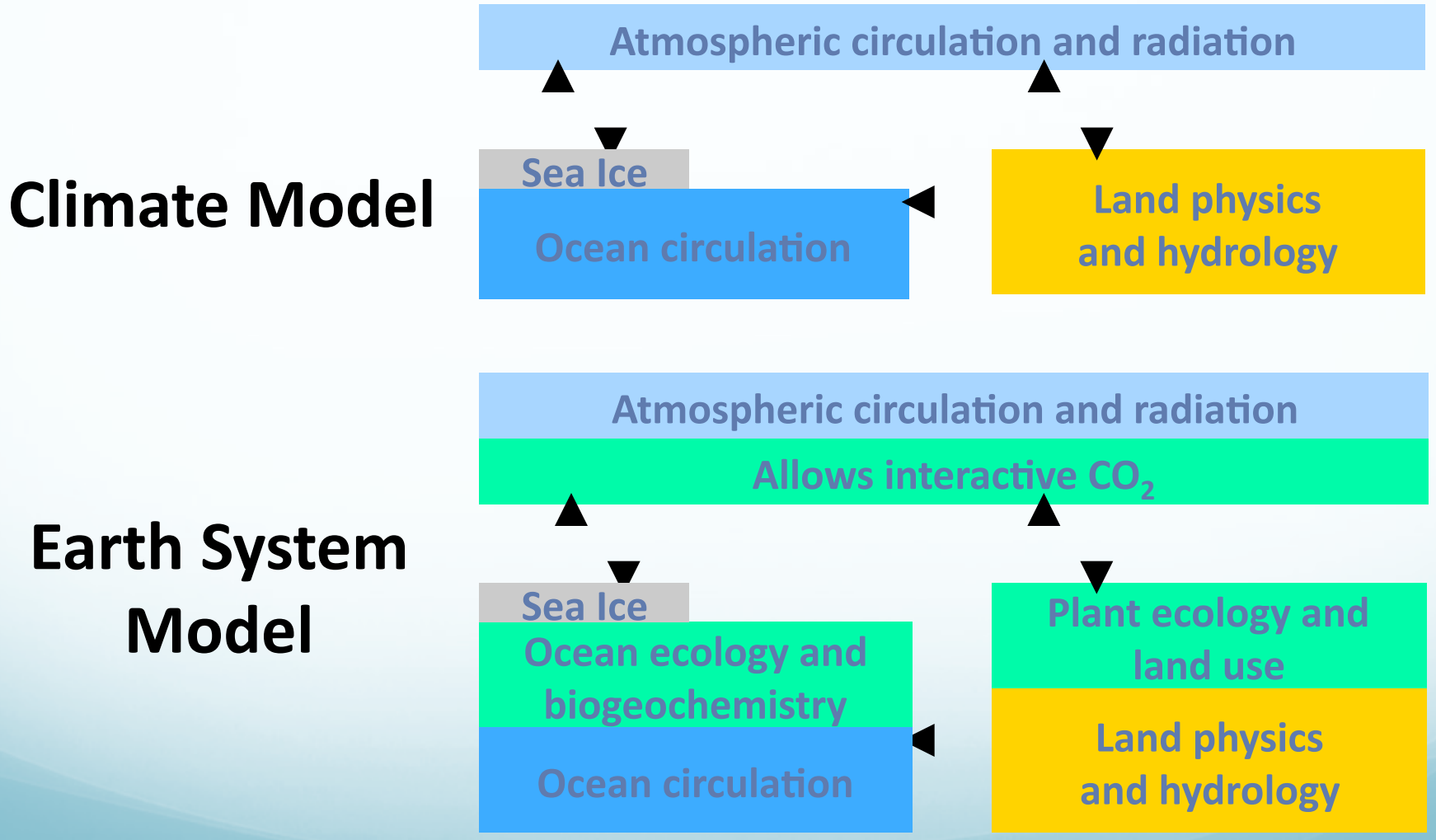

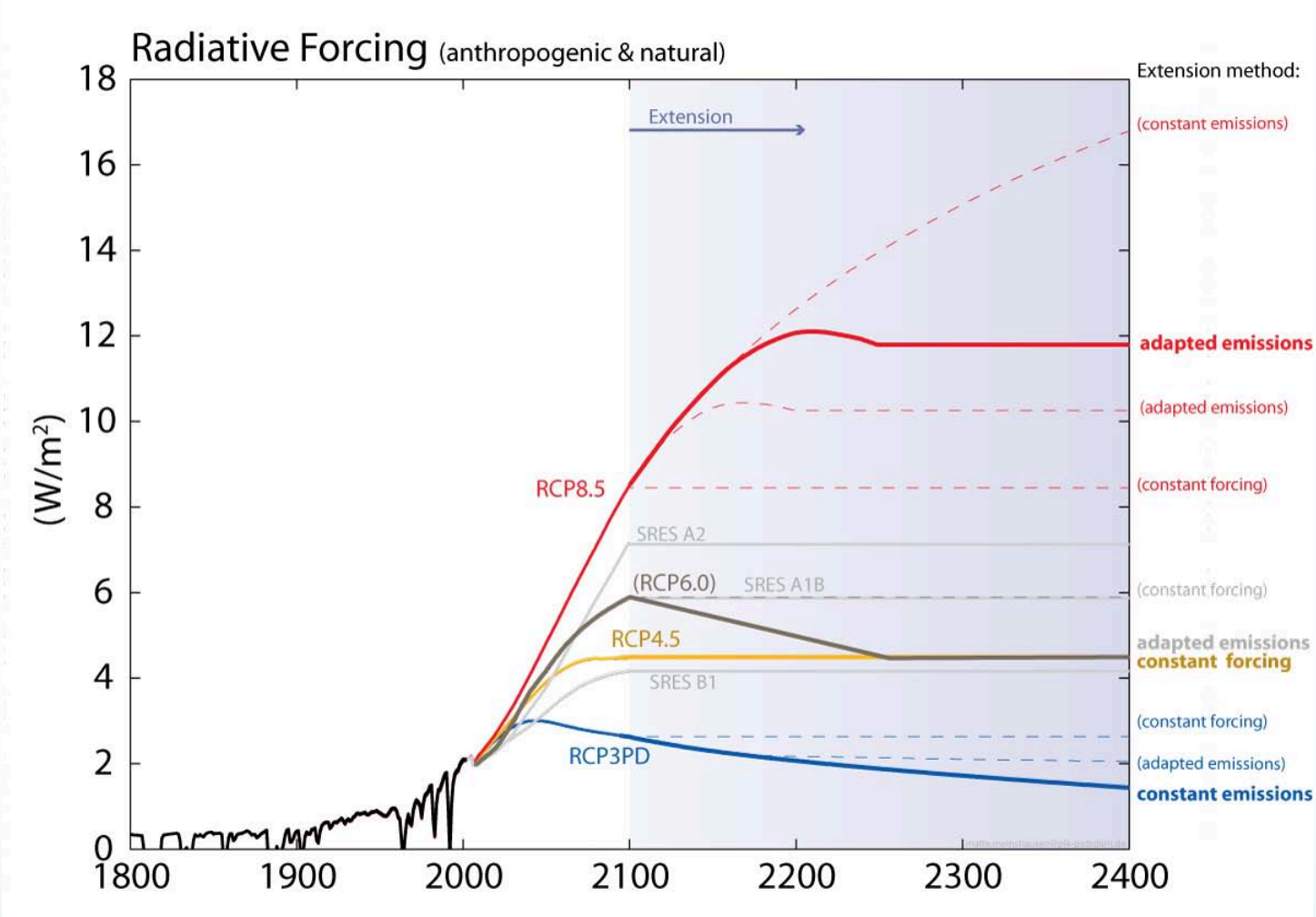

Schematic illustration of radiative forcing in line with a set of extension proposals developed by Detlef van Vuuren, Malte Meinshausen, Steve Smith, and Keywan Riahi. Solid bold lines post-2100 indicate the proposed recommendations by the teleconference participants with dashed lines indicating additional extension possibilities under alternative extension rules.

Change in Mean Wind Speed (m/s)

RCP8.5 (2080-2100) – Historical (1980-2000)

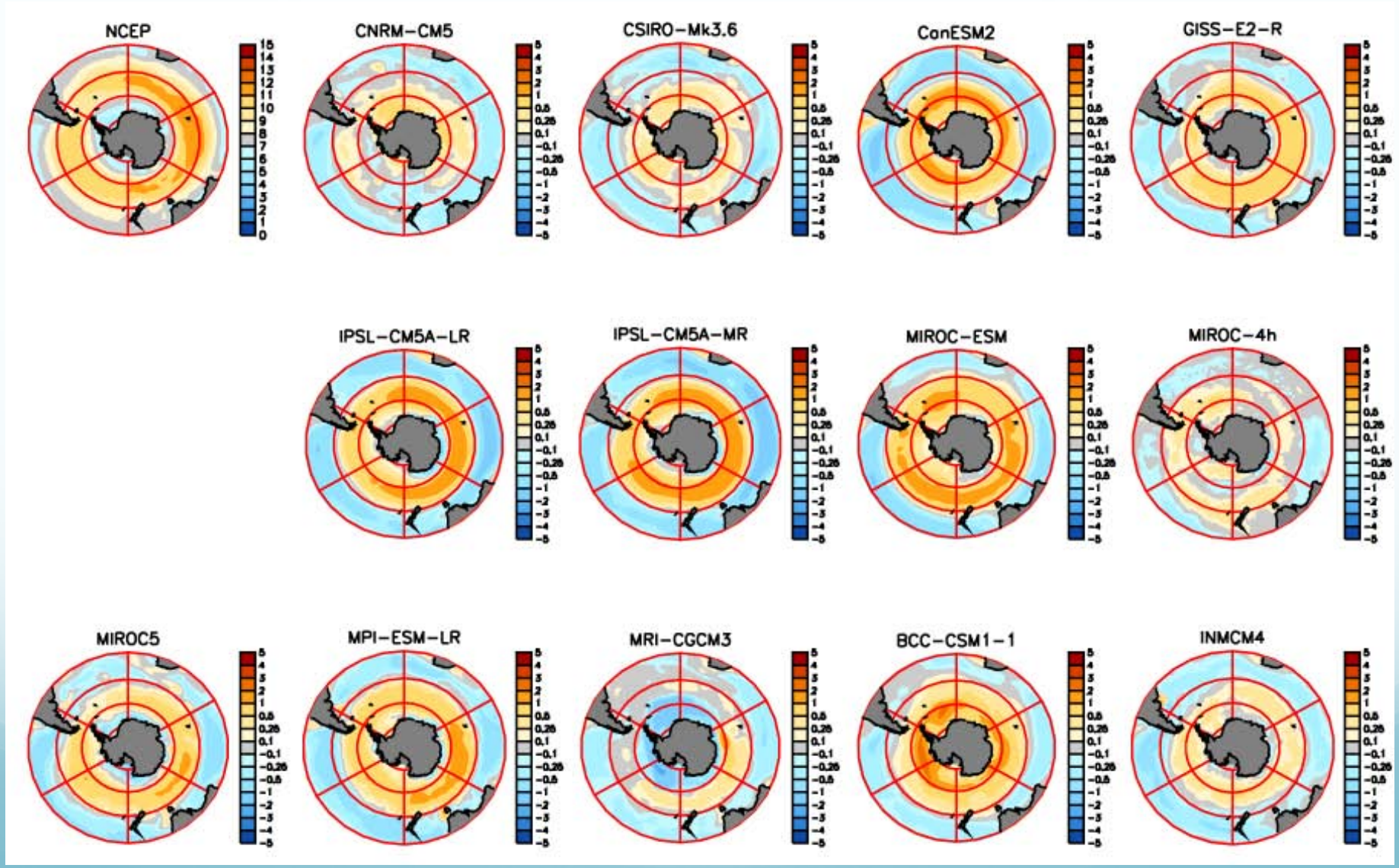

Overall Performance Index $\overline{\overline{I_m^2}}^{v,s}$

courtesy Thomas Reichler & Junsu Kim, Univ. of Utah

A combined measure of how well 21 different global climate models simulate 35 different observed climate features (time averaged, large scale quantities).

Normalized so that the average model score = 1.0; Values less than 1.0 are better.
Lower Values = Smaller Errors (i.e., greater agreement btwn the model simulation & observations)

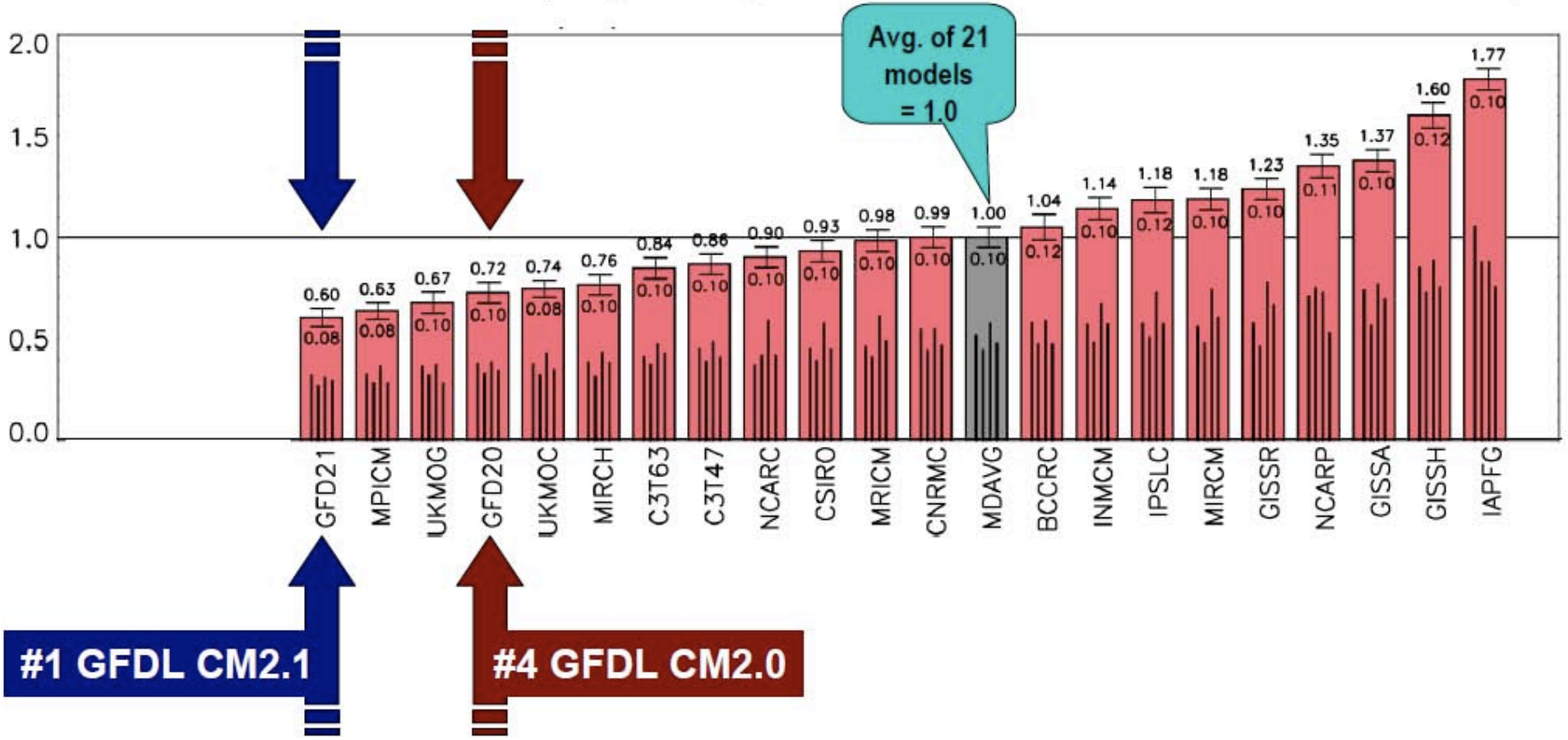

Overall Performance Index $\overline{\overline{I_m^2}}^{v,s}$

courtesy Thomas Reichler & Junsu Kim, Univ. of Utah

A combined measure of how well 21 different global climate models simulate 35 different observed climate features (time averaged, large scale quantities).

Normalized so that the average model score = 1.0; Values less than 1.0 are better.
Lower Values = Smaller Errors (i.e., greater agreement btwn the model simulation & observations)

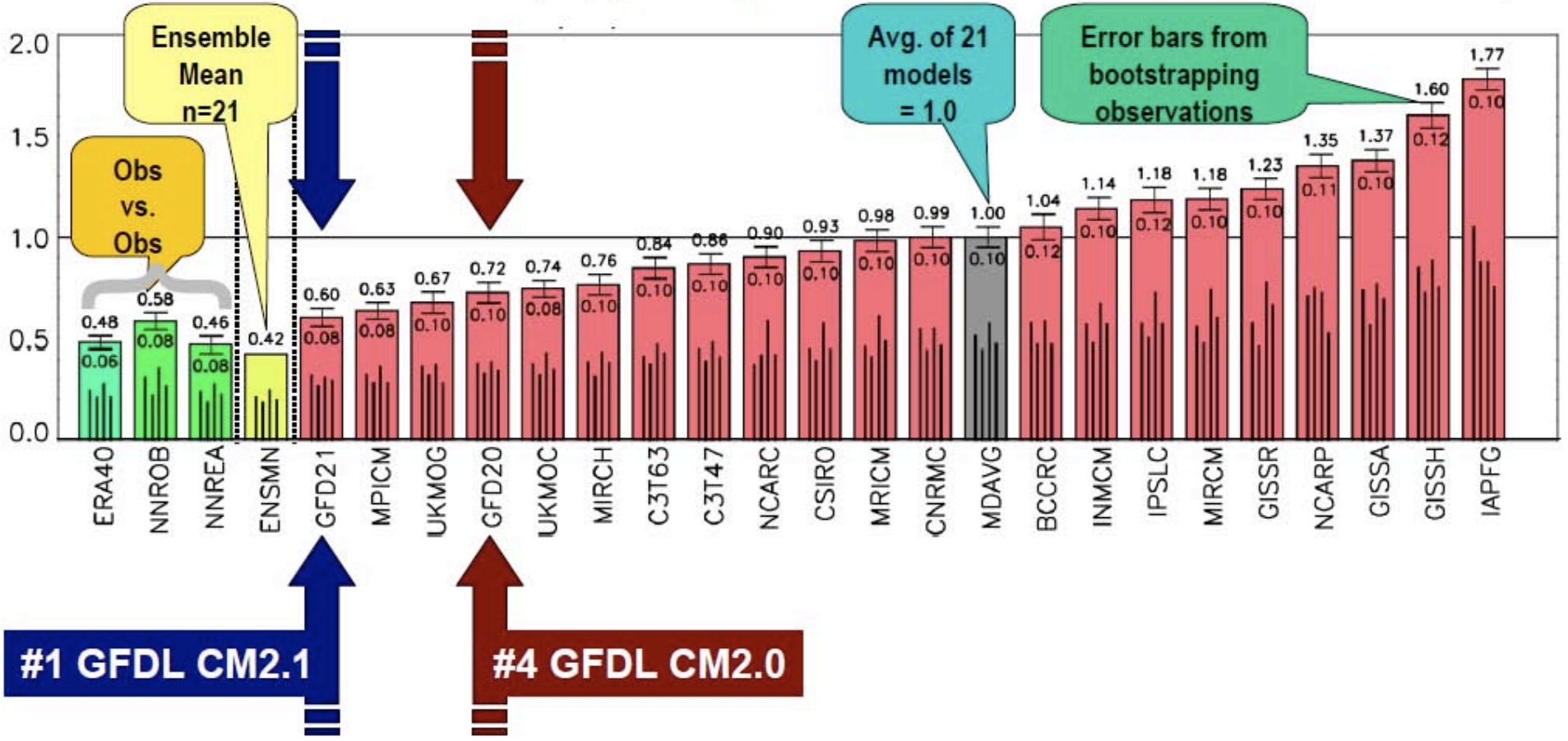

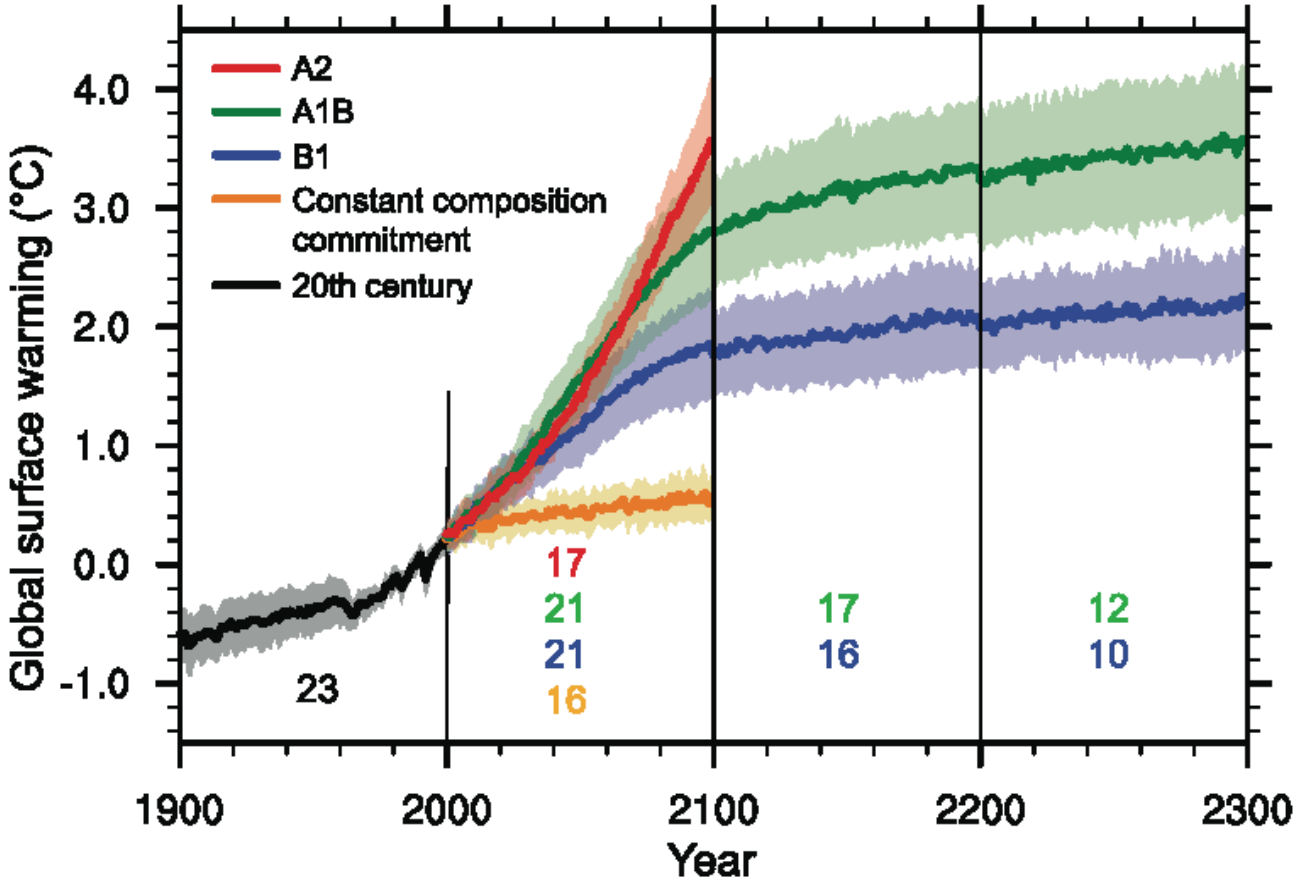

Figure 10.4. *Multi-model means of surface warming (relative to 1980–1999) for the scenarios A2, A1B and B1, shown as continuations of the 20th-century simulation. Values beyond 2100 are for the stabilisation scenarios (see Section 10.7). Linear trends from the corresponding control runs have been removed from these time series. Lines show the multi-model means, shading denotes the ±1 standard deviation range of individual model annual means. Discontinuities between different periods have no physical meaning and are caused by the fact that the number of models that have run a given scenario is different for each period and scenario, as indicated by the coloured numbers given for each period and scenario at the bottom of the panel. For the same reason, uncertainty across scenarios should not be interpreted from this figure (see Section 10.5.4.6 for uncertainty estimates).*

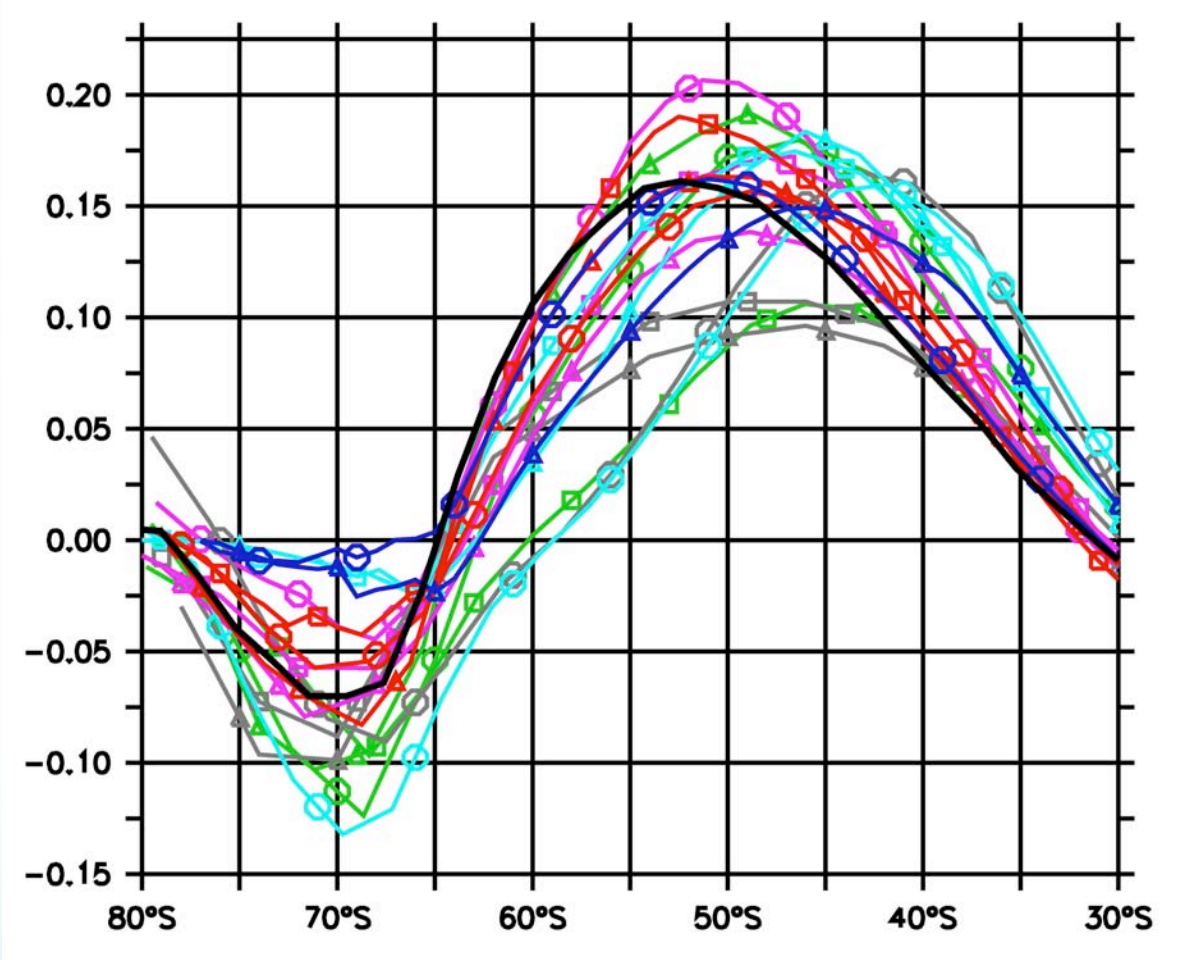

Zonally-averaged wind stress (N/m^2).

Observed (black), GFDL-CM2.1 (blue, circle), GFDL-CM2.0 (blue, triangle)

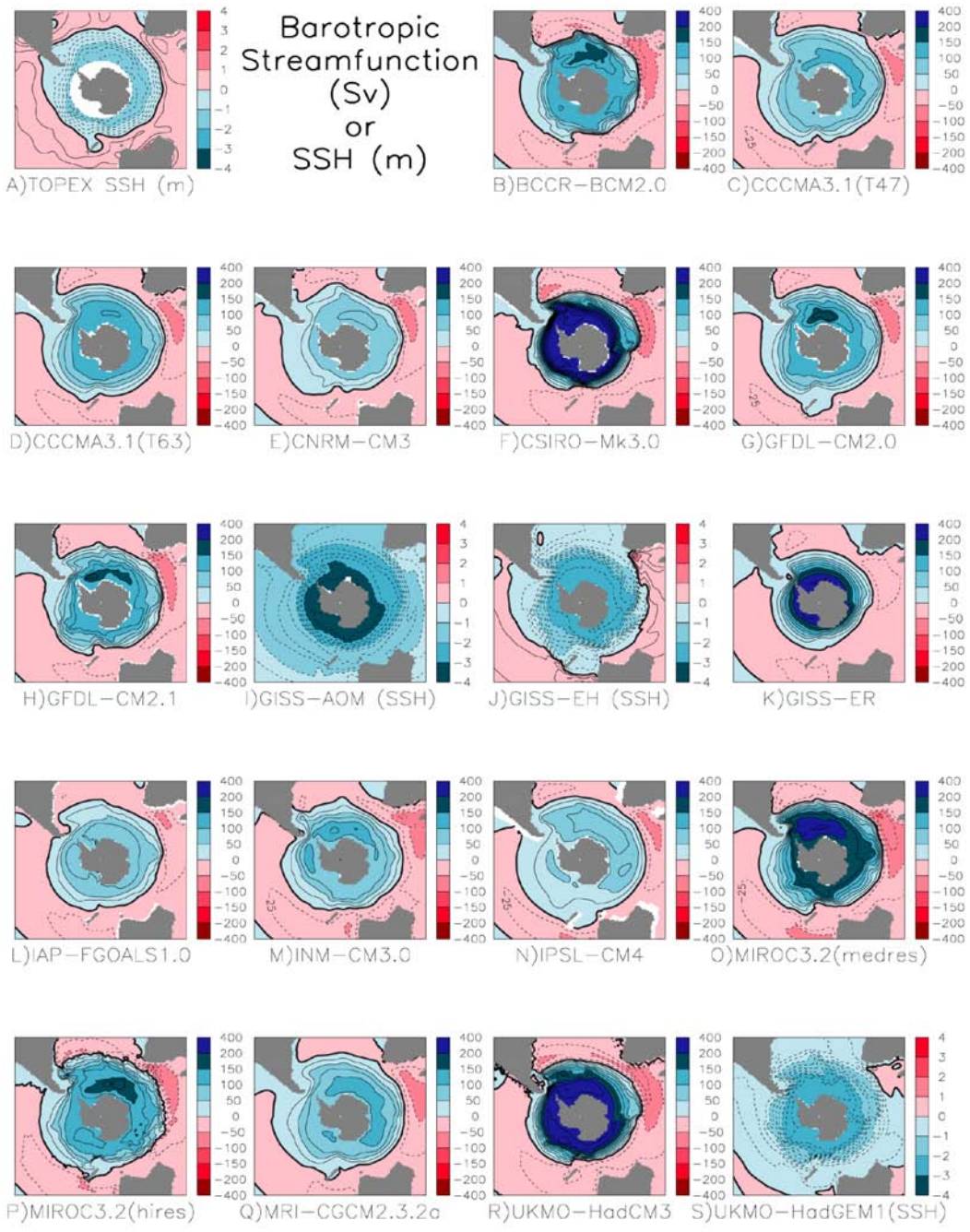

Barotropic Streamfunction (Sv) & Sea Surface Height (m)

Russell et al. (2006a)

Comparison of AR4 Coupled Climate Models

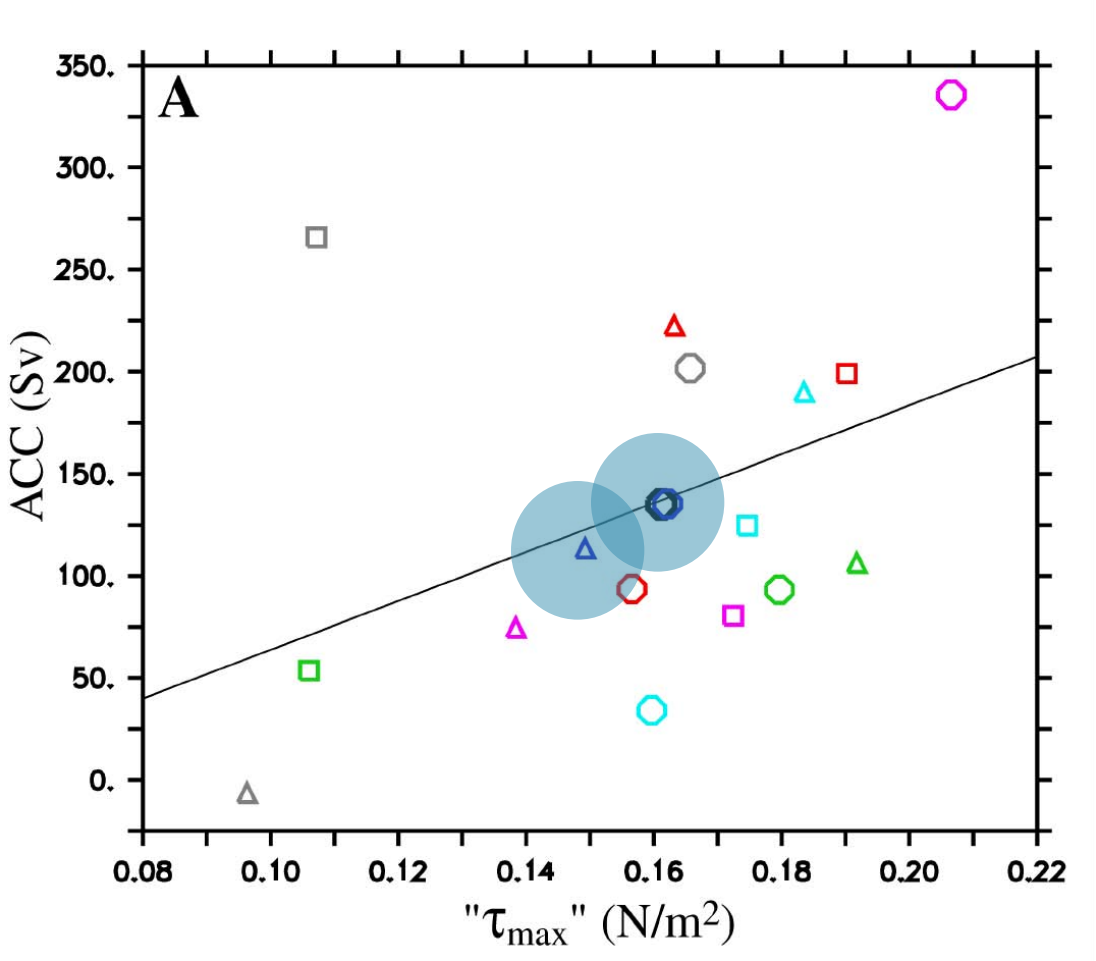

Maximum westerly wind stress vs ACC strength

Russell et al. (2006a)

Southern Ocean Fronts

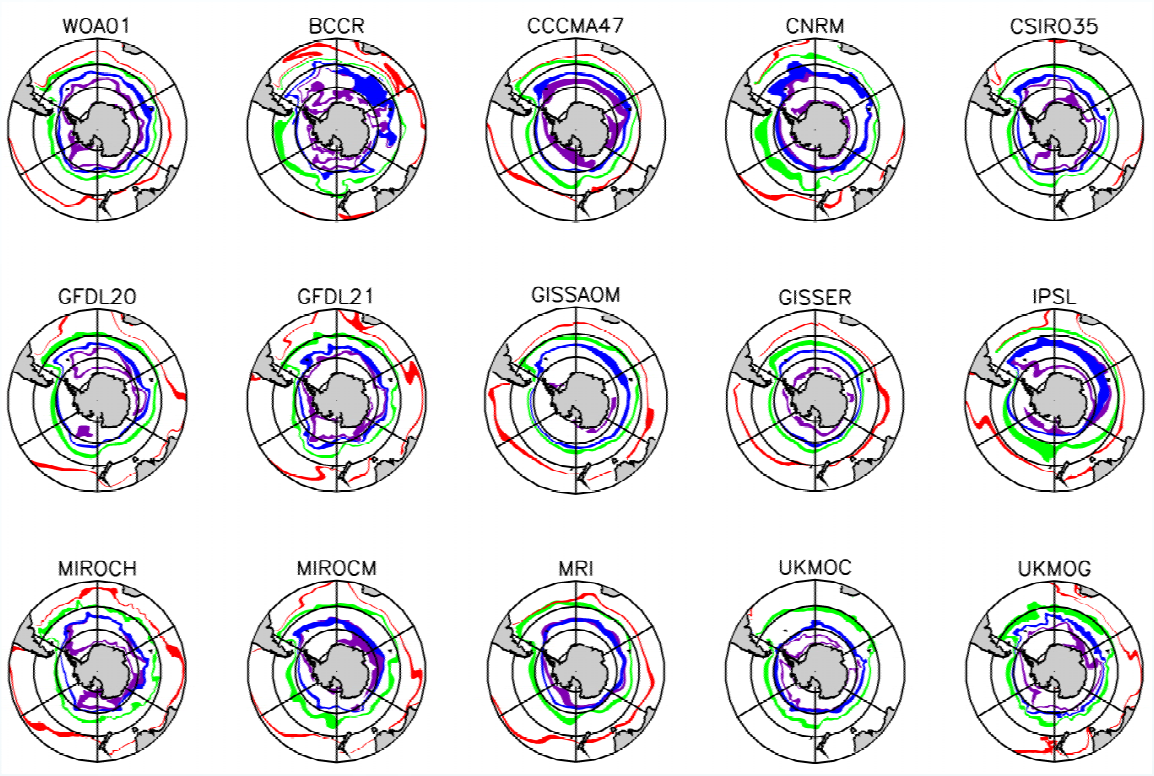

Subtropical Front (salinity between 34.9 and 35.0 at 100m)

Subantarctic Front (temperature between 4°C and 5°C at 400m)

Polar Front (temperature minimum in the upper 200 meters between 1°C and 2°C)

Southern Boundary of the ACC (sigma-0 between 27.55 and 27.65)

All definitions are after Orsi et al. (1995).

Temperature Error at 30°W

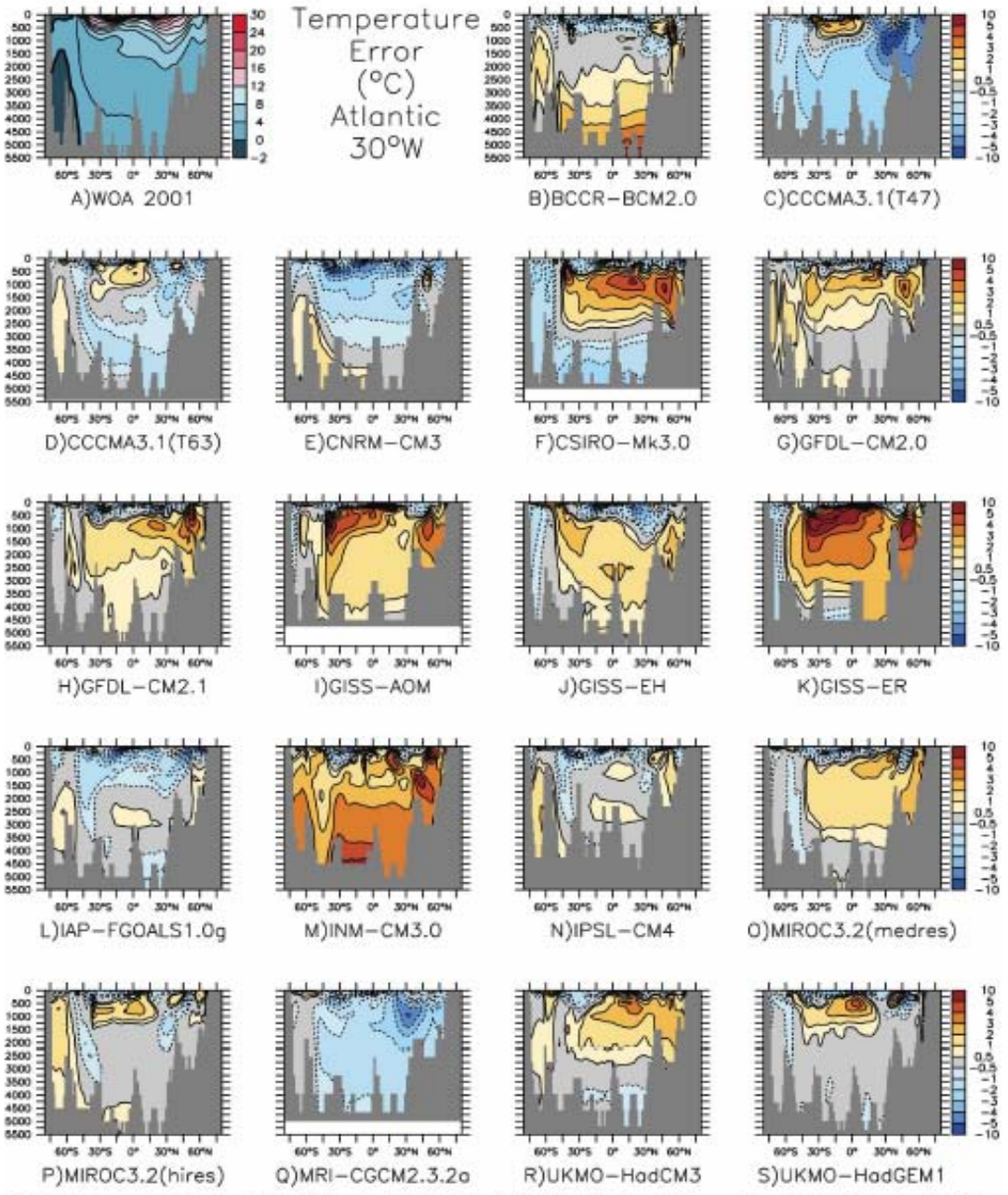

FIG. 7. Temperature differences from (a) the observations along 30°W from 18 of the IPCC ocean models. Positive values indicate the model is warmer than observed.

Types of Circulation Errors

1. About Right (ACC strength and position, Westerly Winds, Freshwater and heat fluxes, NADW heat and salt transport into the Southern Ocean) - GFDL CM2.1, MIROC3.2(hires)

2. Wind stress errors that lead to incorrect ACC transports
   a) Too high wind stress over ACC (CSIRO-Mk3.0, MIROC(medres), UKMO-HadGEM1
   b) Too weak wind stress produce weak ACC (CNRM and IAP)
   c) Equatorward displacement of strong winds (GFDL CM2.0, BCCR-BCM2.0, MRI-CGM2.3.2a, both CCMA models)
   d) Equatorward displacement of weak winds (GISS-AOM, GISS-ER)

3. Incorrect formation of NADW
   a) NADW too warm, fresh or weak (INM-CM3.0, IPSL-CM4)
   b) NADW too large (UKMO-HadCM3)

Maximum Zonally-Averaged Sea-Ice Cover

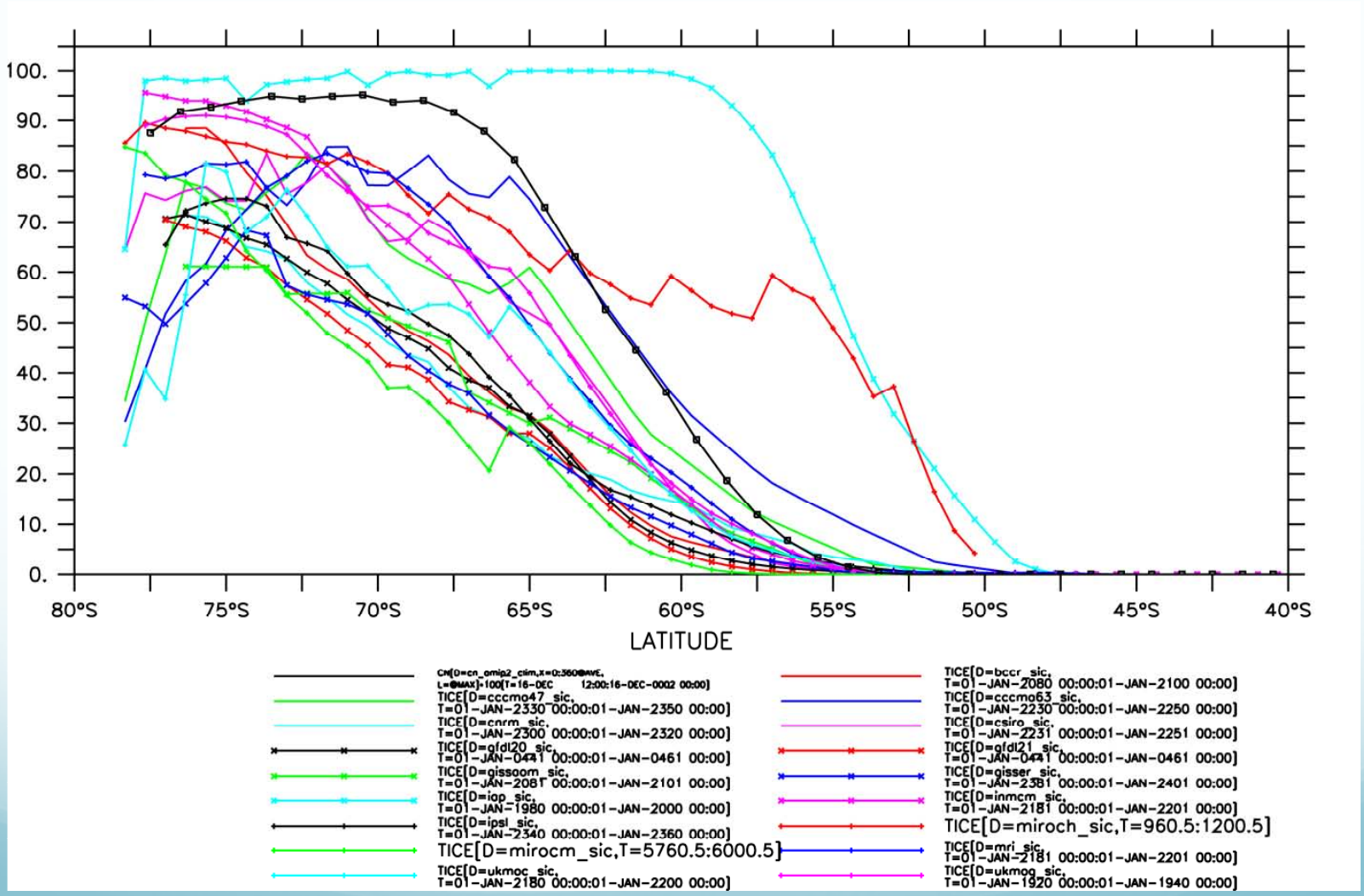

RMS Error for the Models

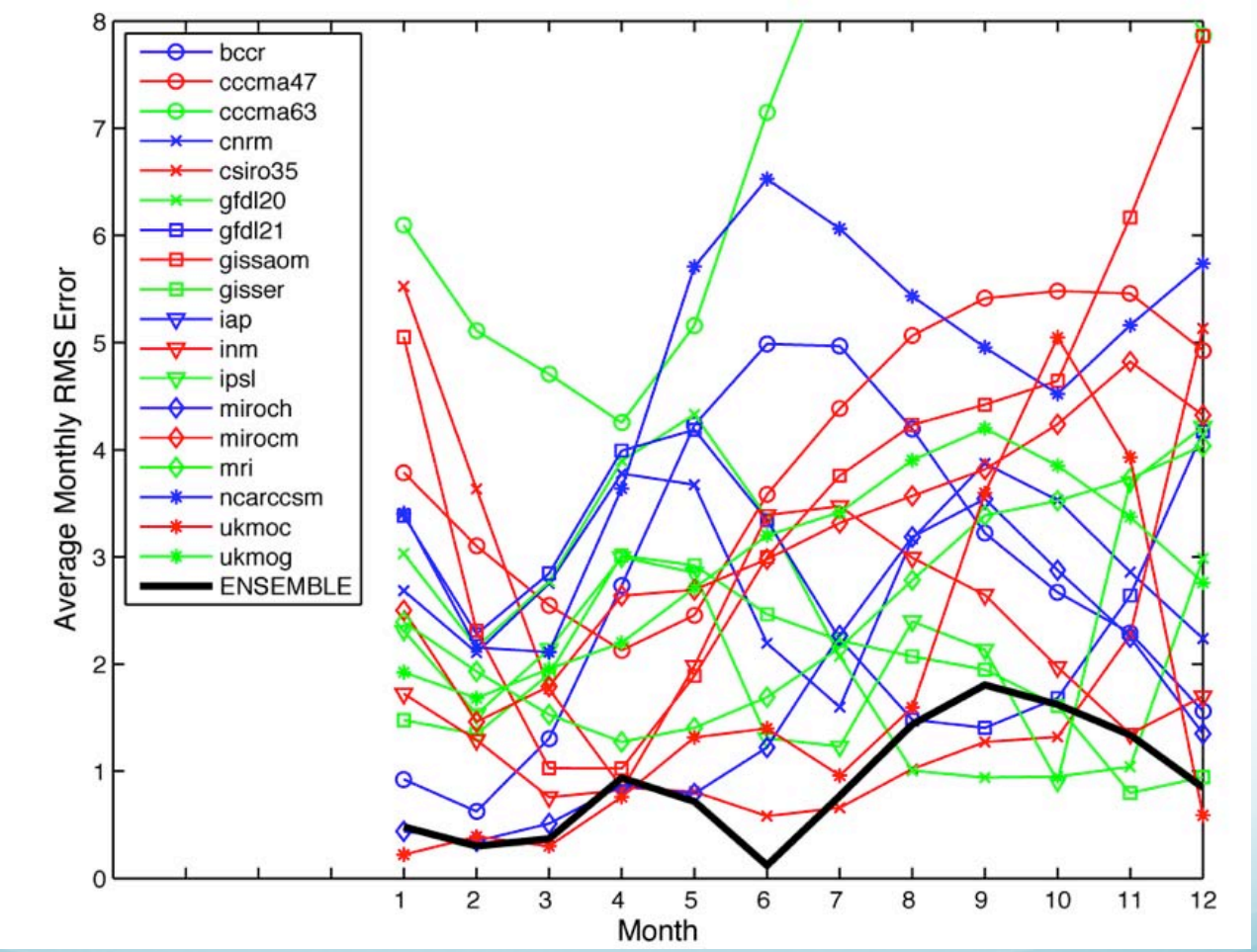

Season Cycle for the Models

Annual Mean RMS For the Preindustrial Control

BCCR	2.8094	
CCCMA47	4.0274	
CCCMA63		7.4197 (not shown)
CNRM	2.8718	
CSIRO35	2.0707	
GFDL20	2.3797	
GFDL21	2.8040	
GISSAOM	3.7827	
GISSER	1.8940	
IAP		23.912 (not shown)
INM	2.0082	
IPSL	2.3100	
MIROCH	1.6376	
MIROCM	3.1794	
MRI	2.4868	
NCARCCSM	4.6182	
UKMOC	1.6758	
UKMOG	2.9309	
ENSEMBLE	**0.8963**	

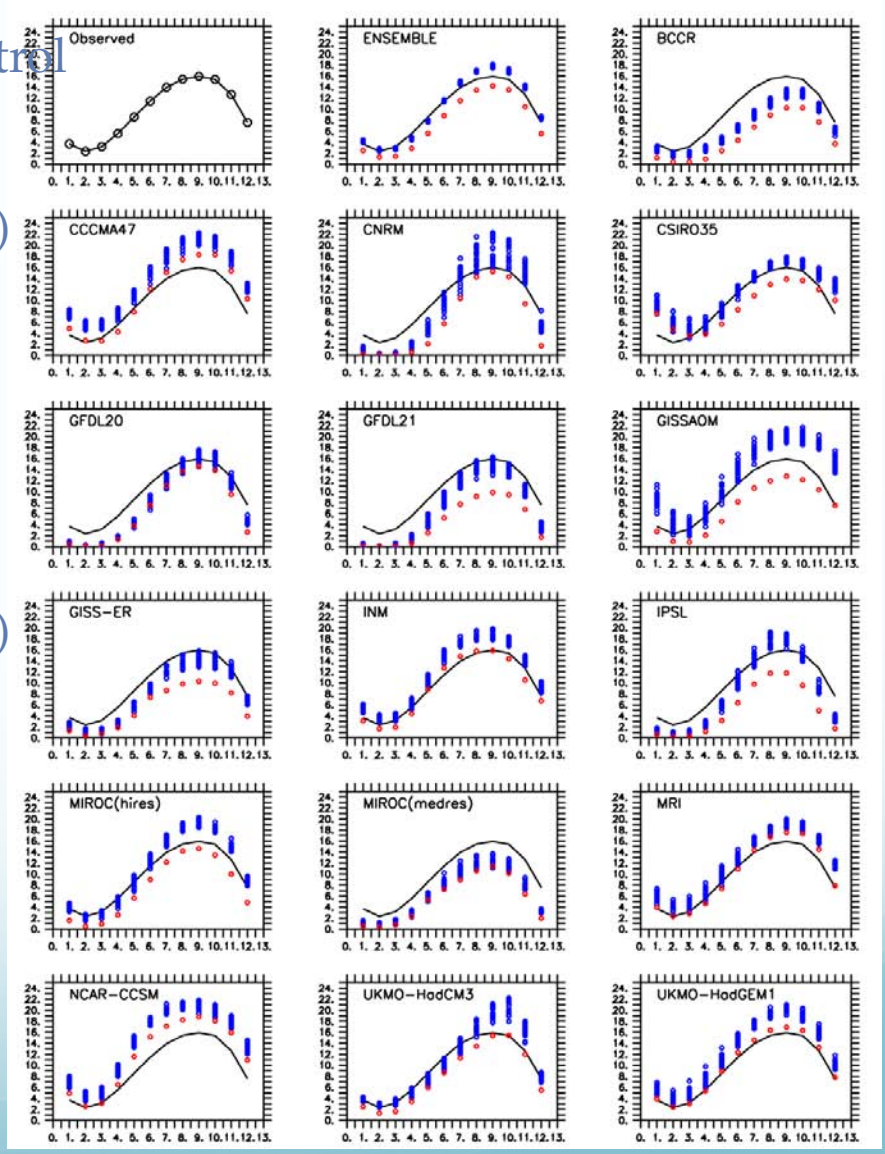

Annual Mean Sea Ice Coverage During the Preindustrial Control Simulation

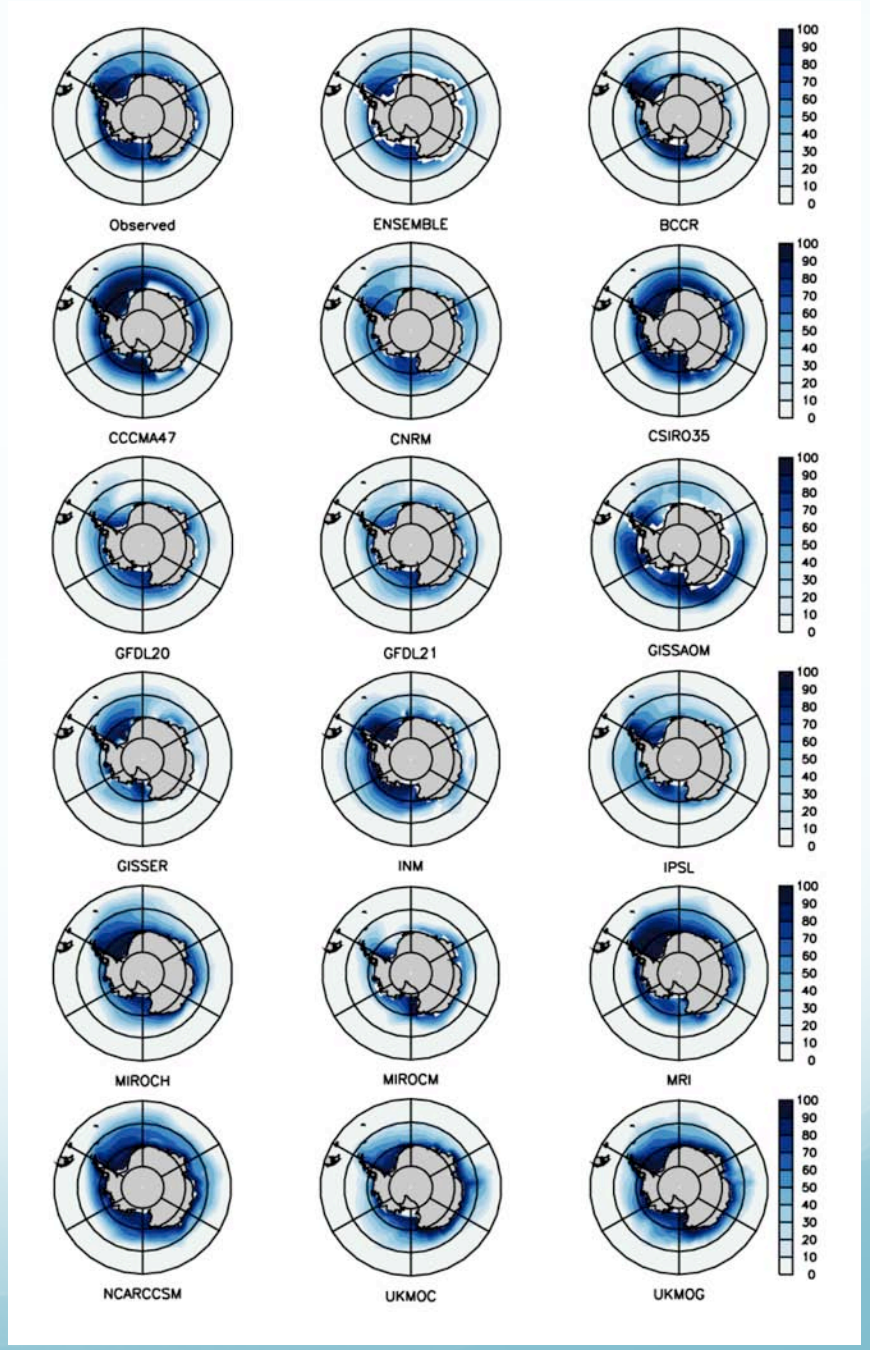

The Southern Ocean in a Warming World

Atmospheric Warming

Globally-averaged, relative to the Pre-Industrial Control

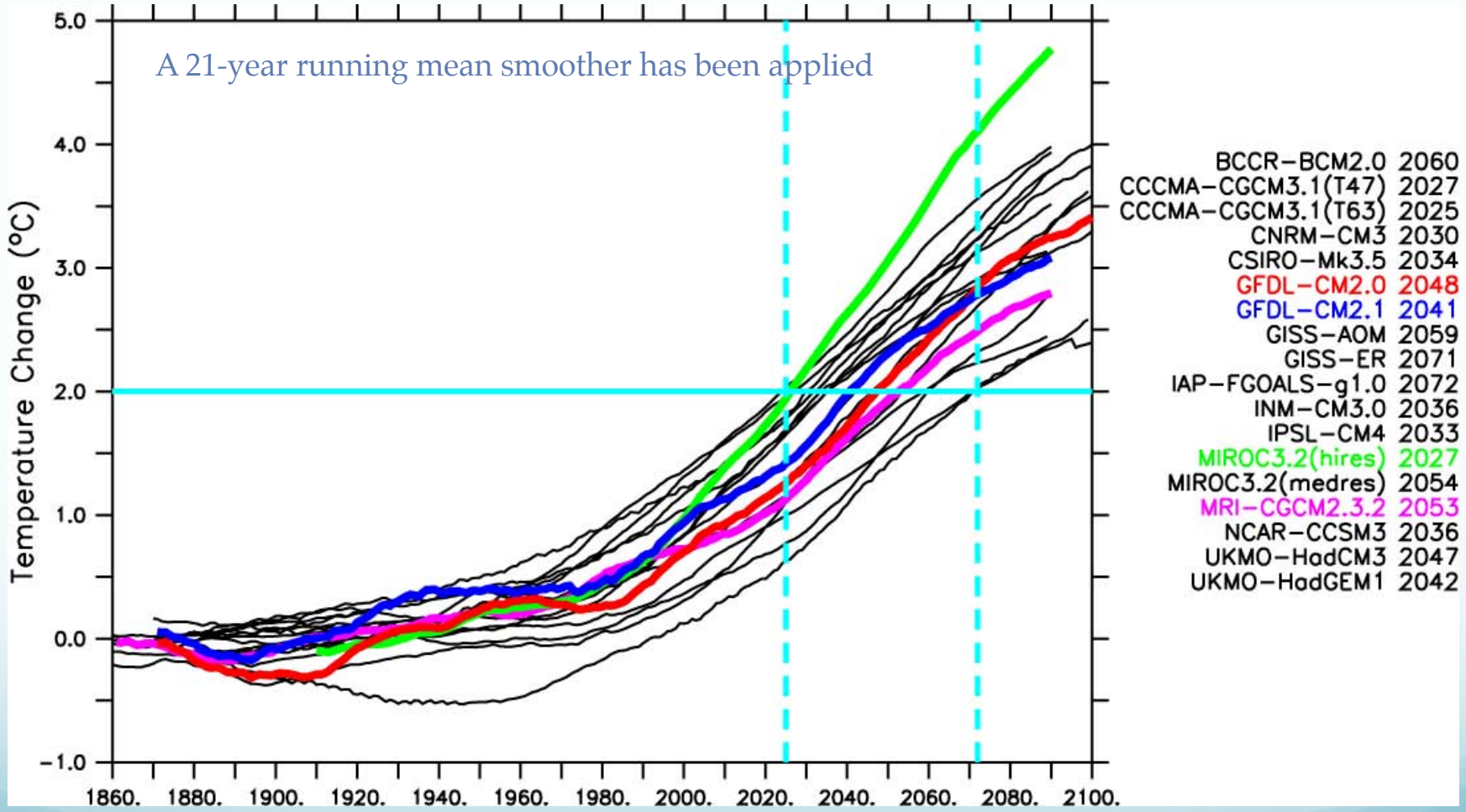

Antarctic Ice Area Anomaly

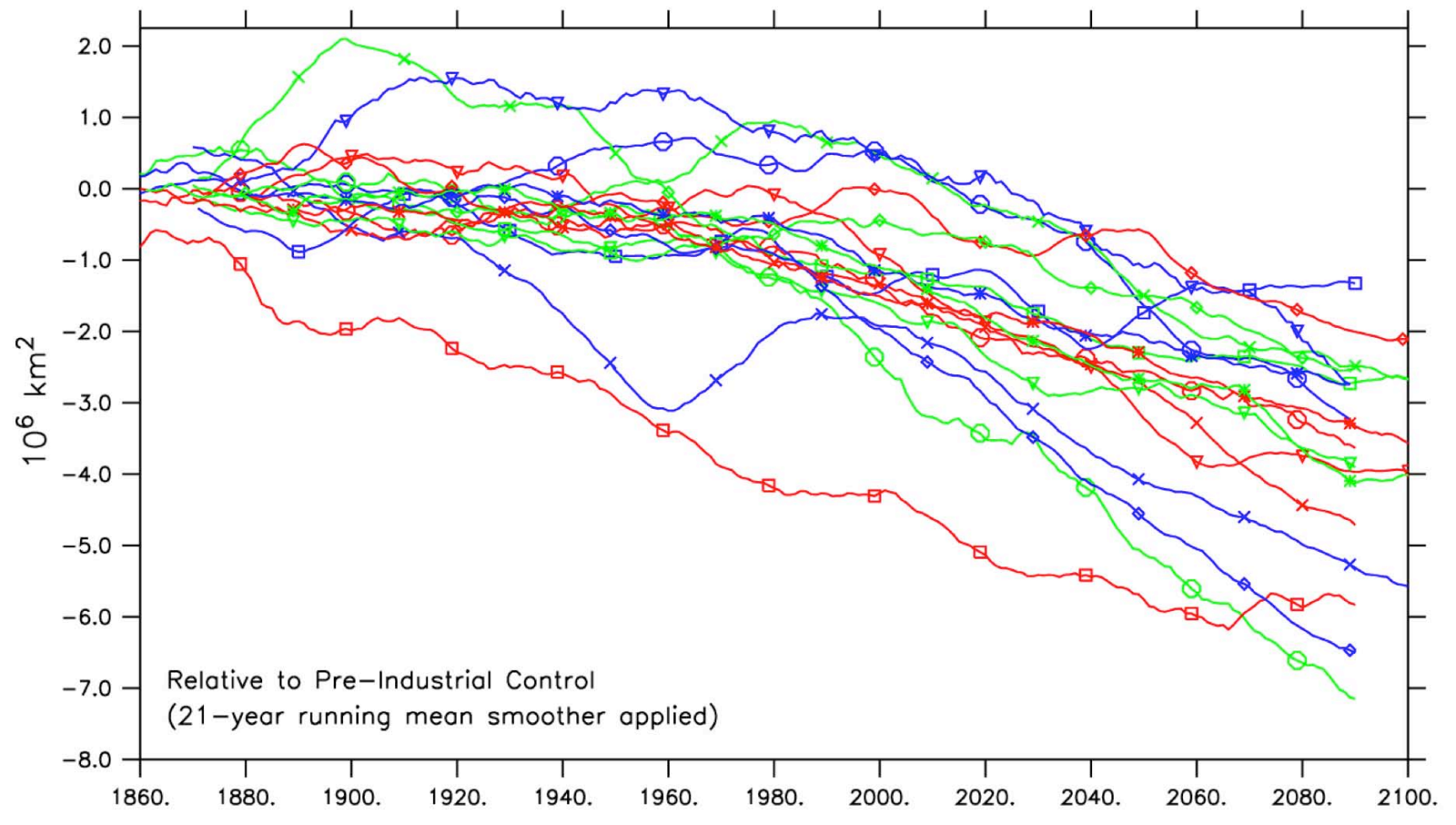

Ross Sea Ice Area Anomaly

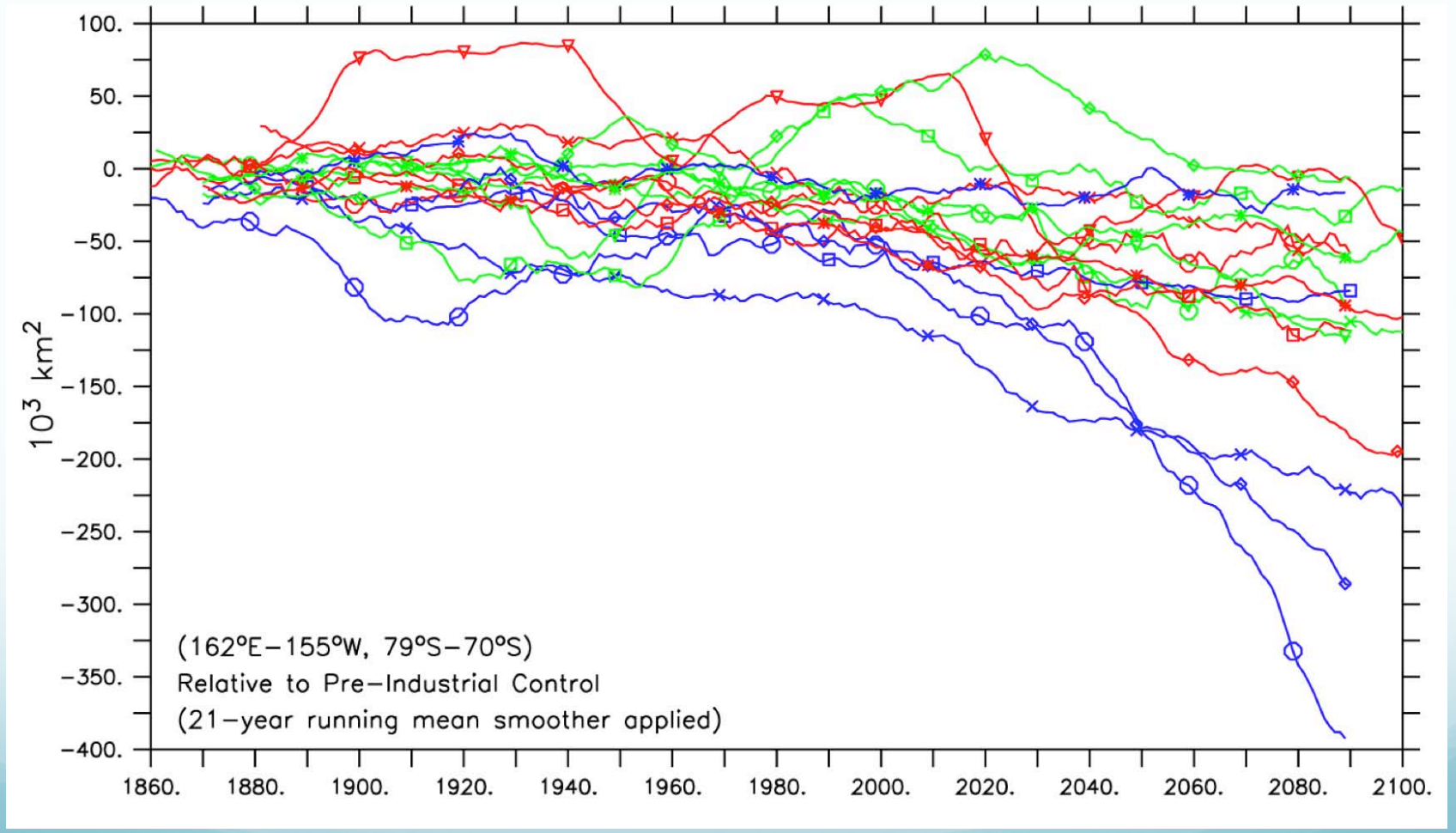

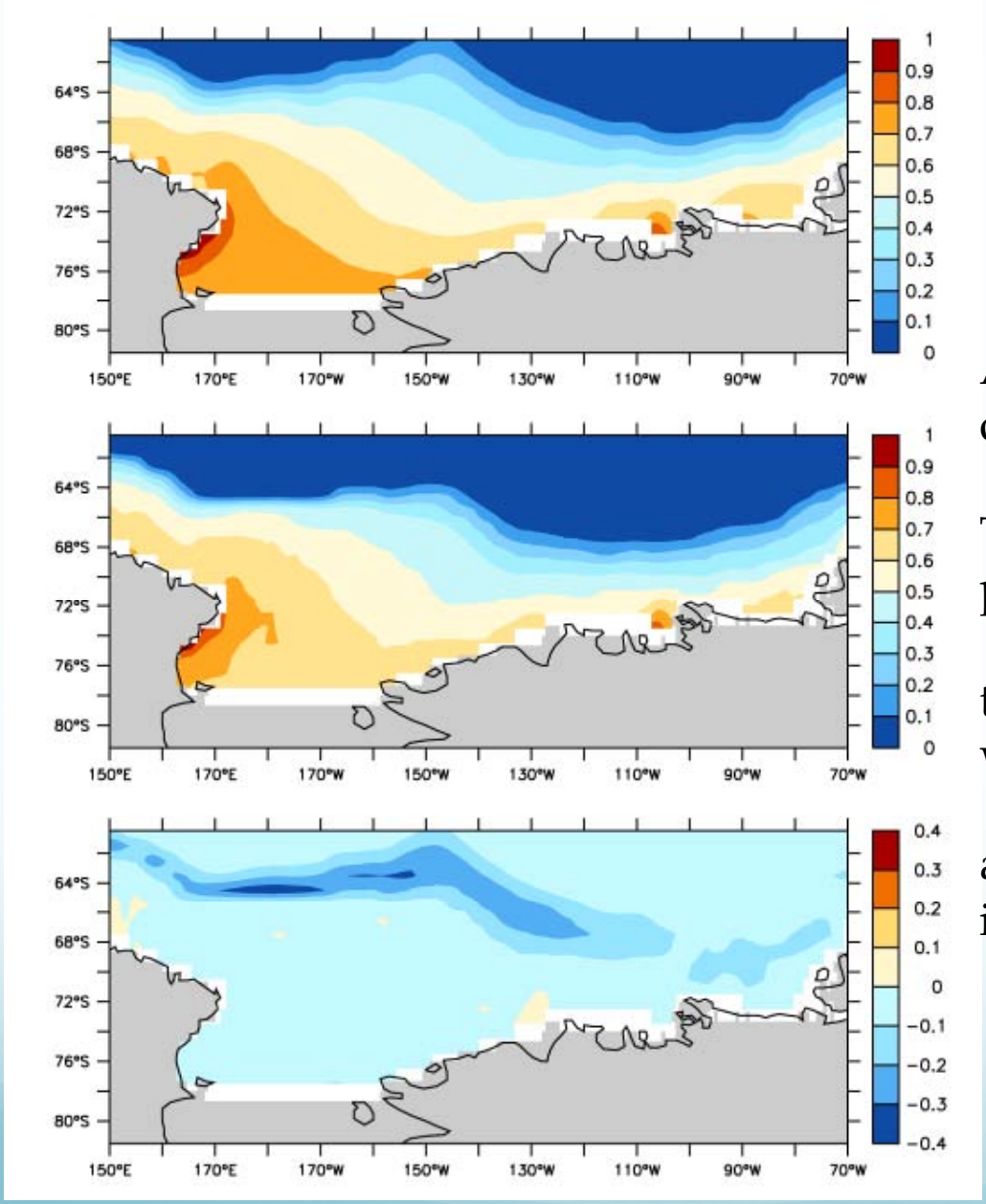

Average area coverage of all sea ice over the Ross Sea.

The upper panel is for the reference period (1981-2000),

the middle panel is for the year of 2° warming (2070),

and the bottom panel is the difference in fractional coverage

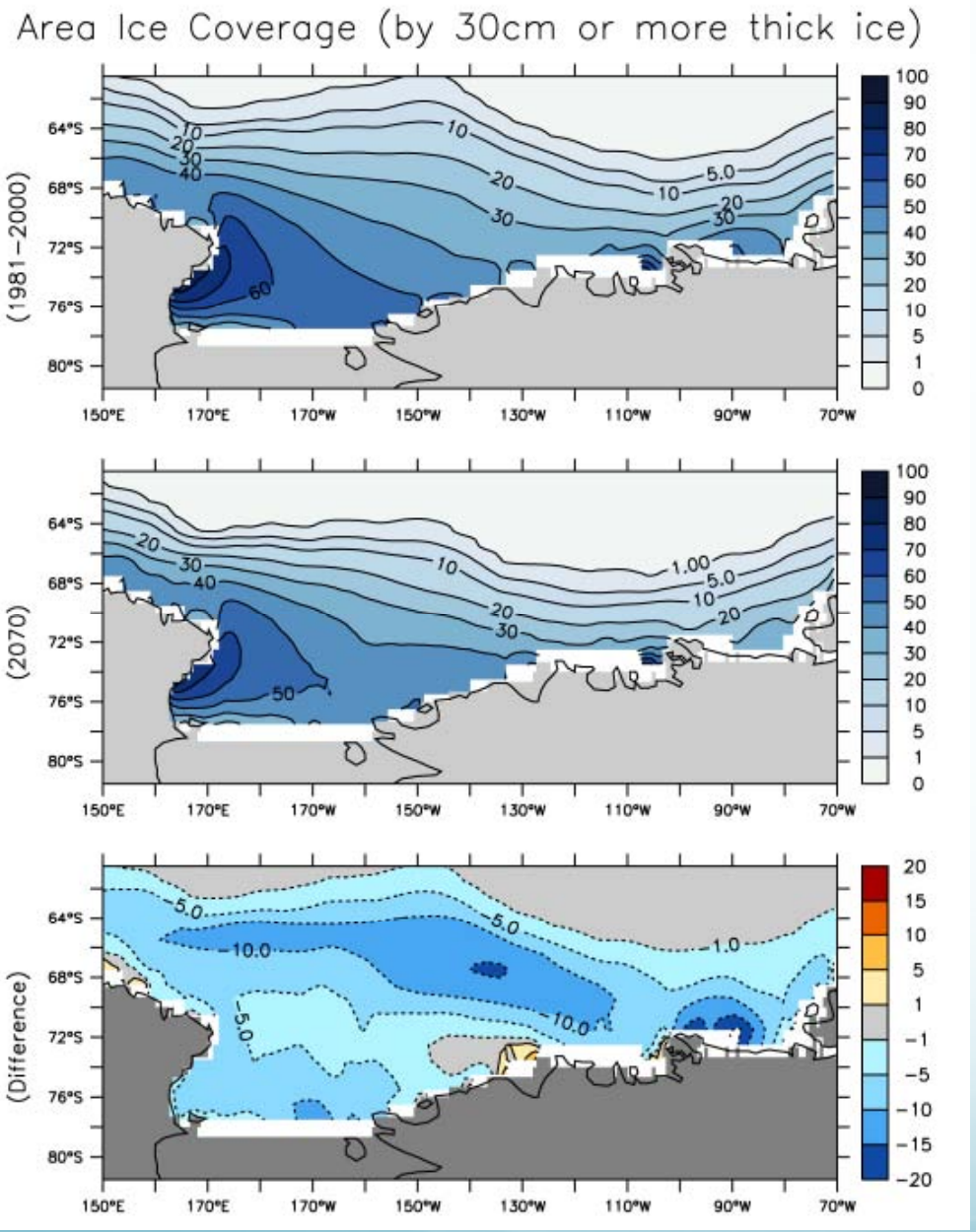

For ice thicker than 30 cm.

Average area coverage of all sea ice over the Ross Sea.

The upper panel is for the reference period (1981-2000),

the middle panel is for the year of 2° warming (2070),

and the bottom panel is the difference in fractional coverage

Change in Ensemble Annual Mean

Sea Ice Coverage (%)

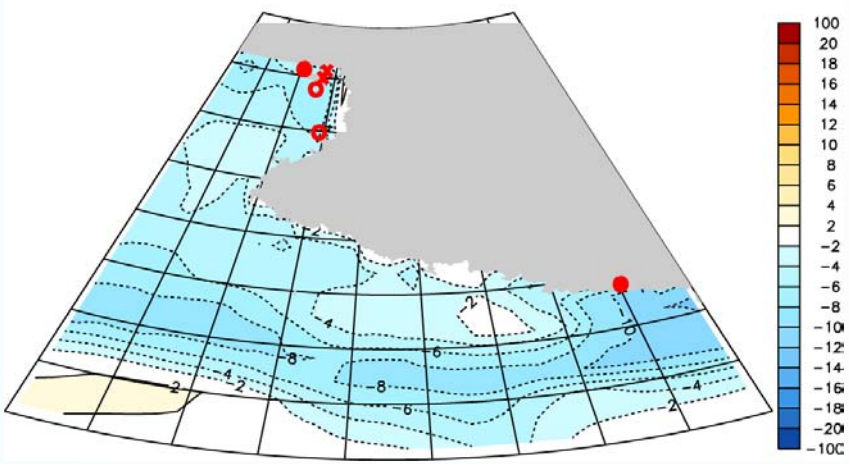

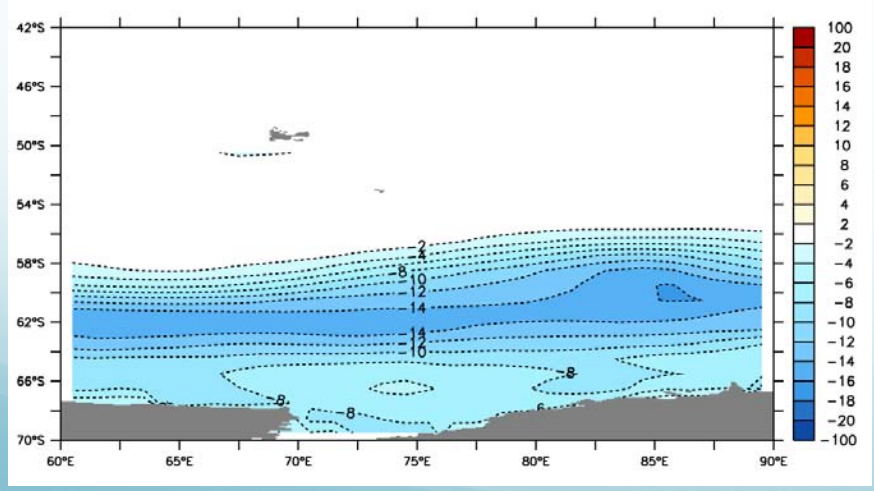

Sea Ice Thickness (cm)

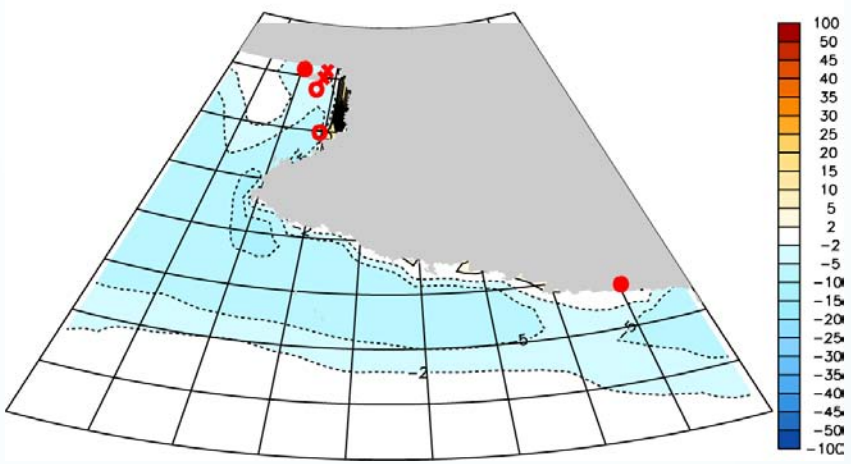

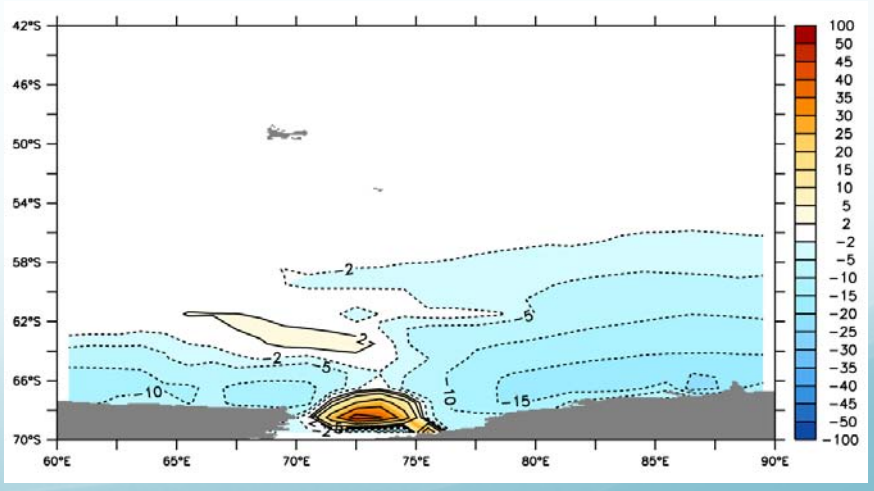

Change in Ensemble Annual Mean

Over the Western Ross Sea

Precipitation (cm/yr)

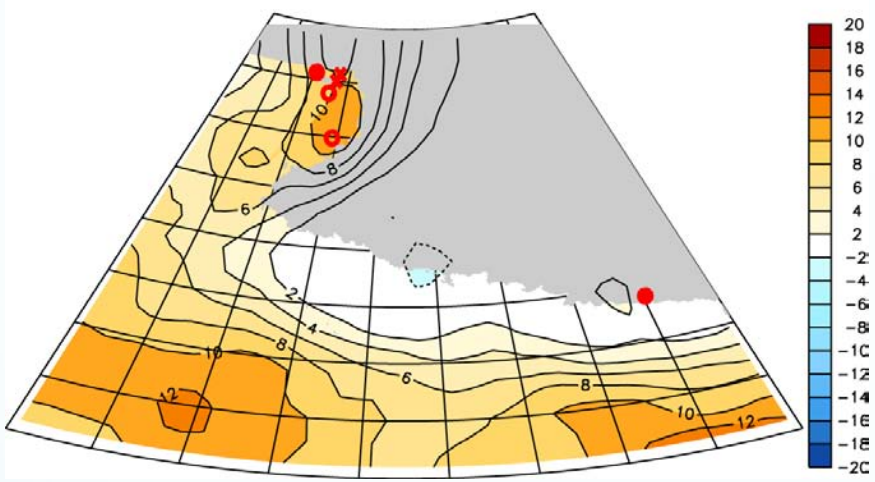

Zonal Wind Stress ($10^{-3}N/m^2$)

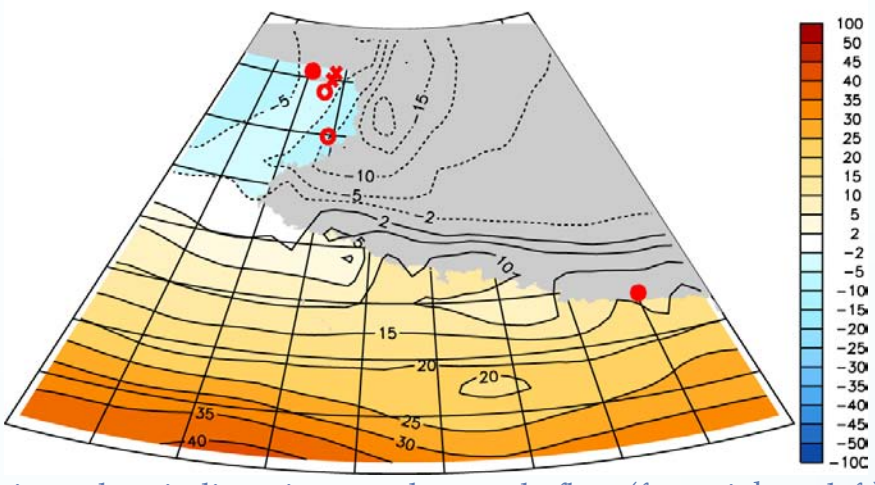

Positive values indicate increased westerly flow (from right to left)

Surface Air Temperature (°C)

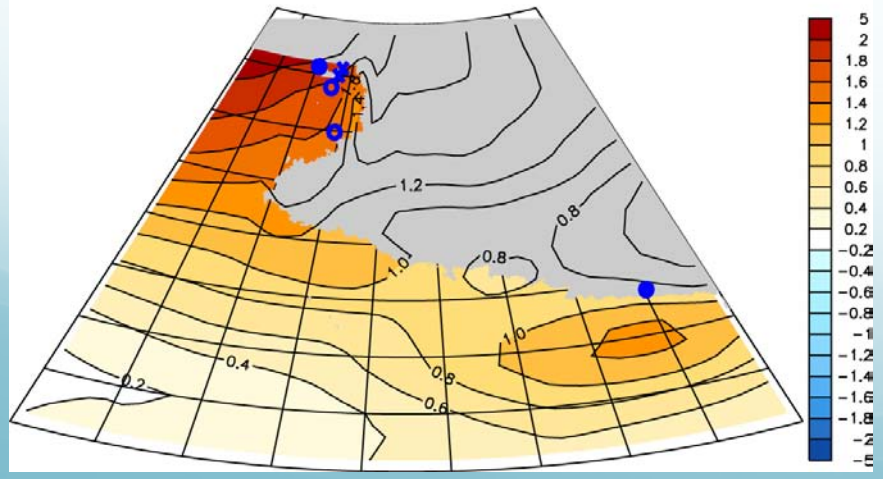

Sea Surface Temperature (°C)

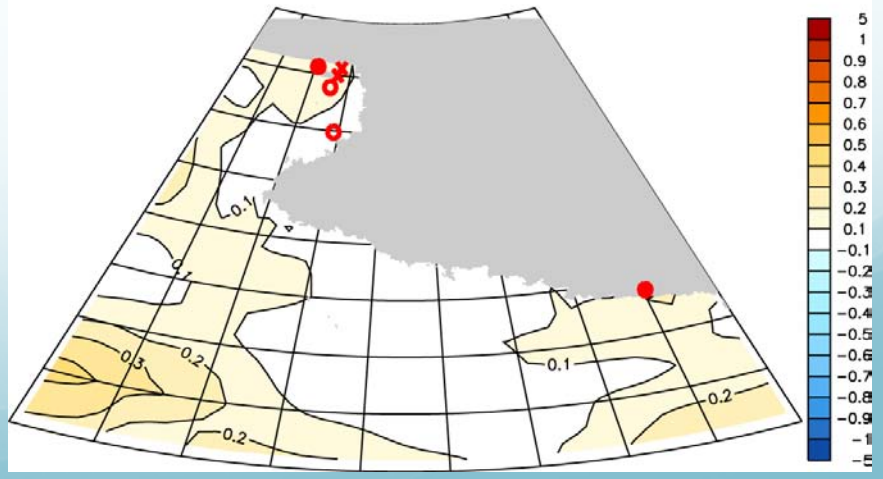

Change in Ensemble Annual Mean

Sea Ice Coverage (%)

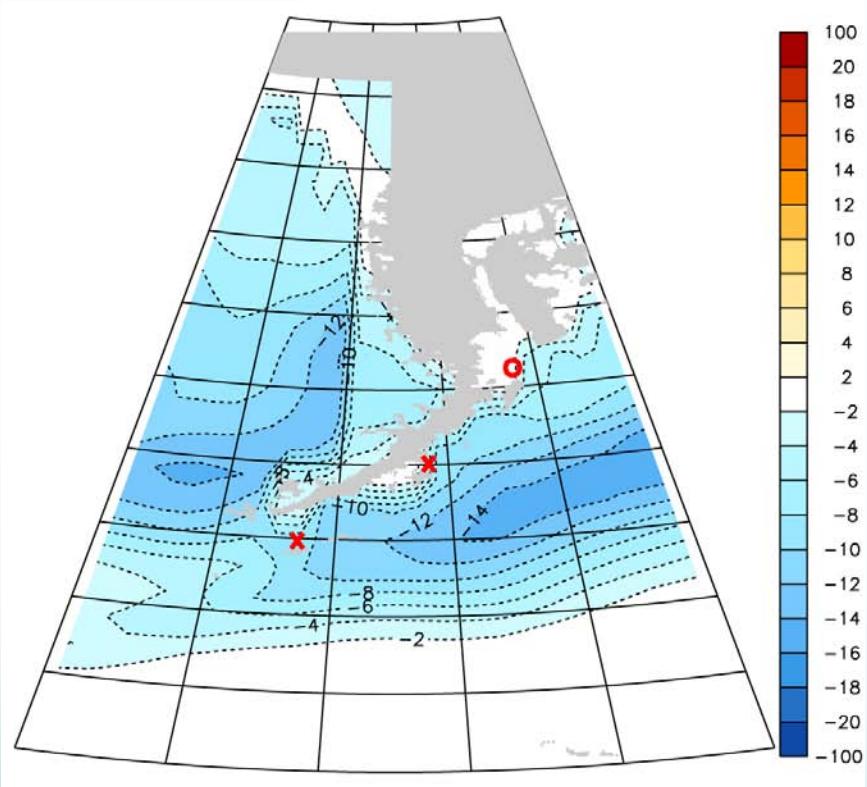

Sea Ice Thickness (cm)

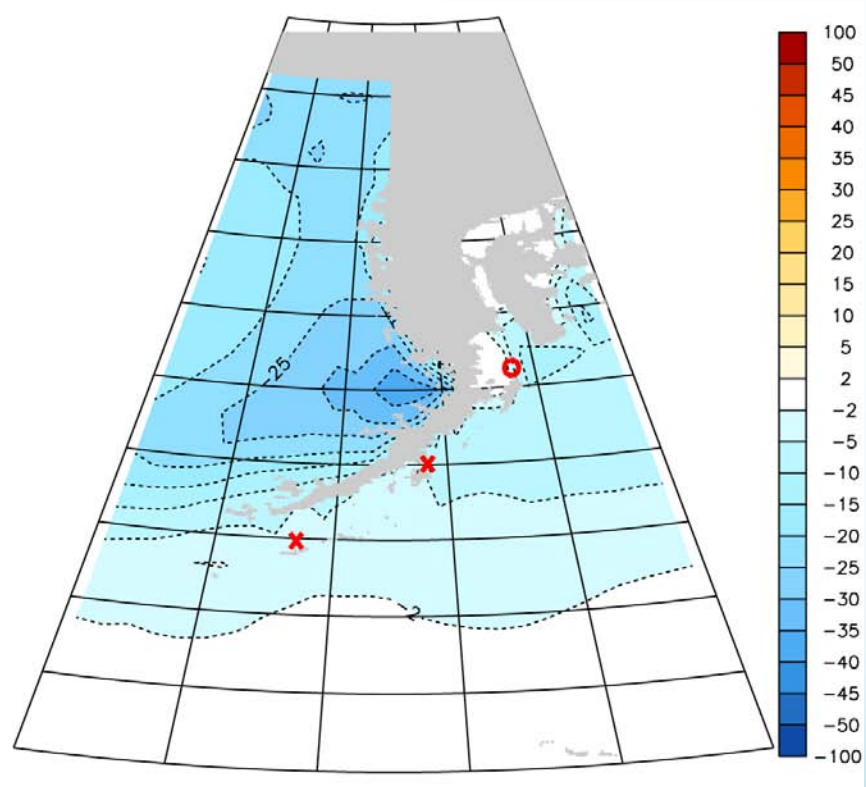

Change in Ensemble Annual Mean

Over the Antarctic Peninsula

Precipitation (cm/yr)

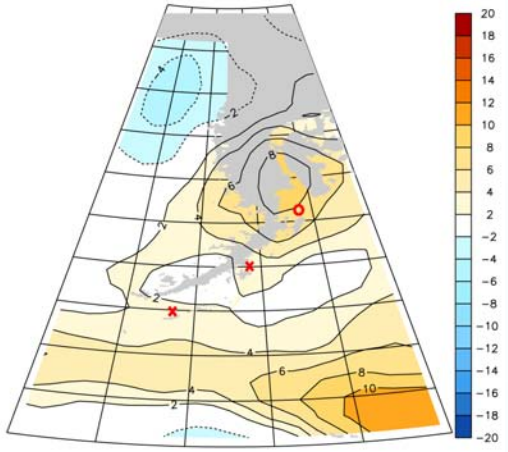

Zonal Wind Stress ($10^{-3}N/m^2$)

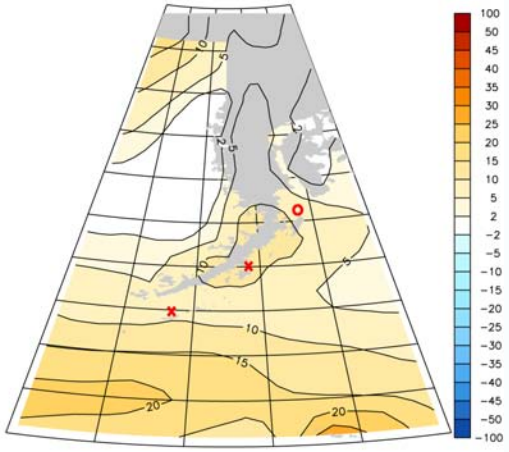

Positive values indicate increased westerly flow (from right to left)

Surface Air Temperature (°C)

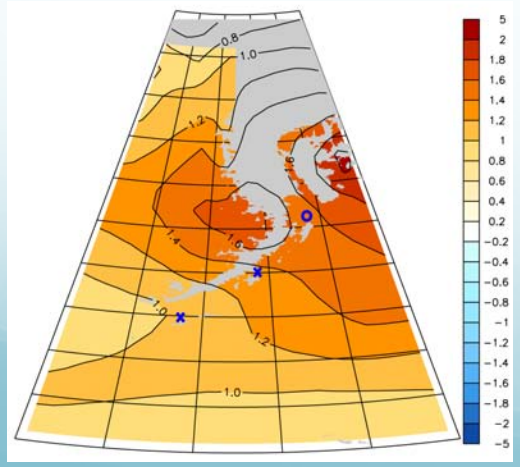

Sea Surface Temperature (°C)

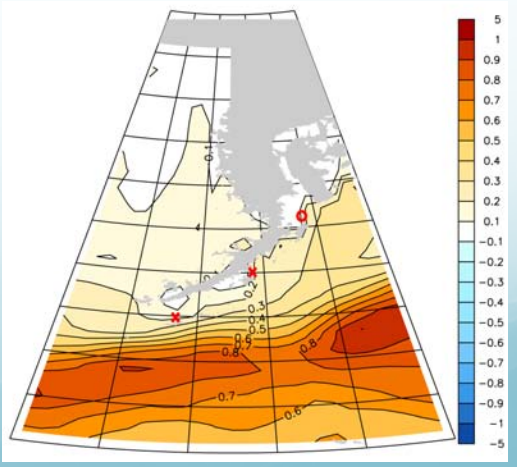

Mesoscale-Resolving Global Climate Models

Model Response to SRESA1B Scenario

(CO_2 increases to 700+ppm @ year 2100, steady to 2300)

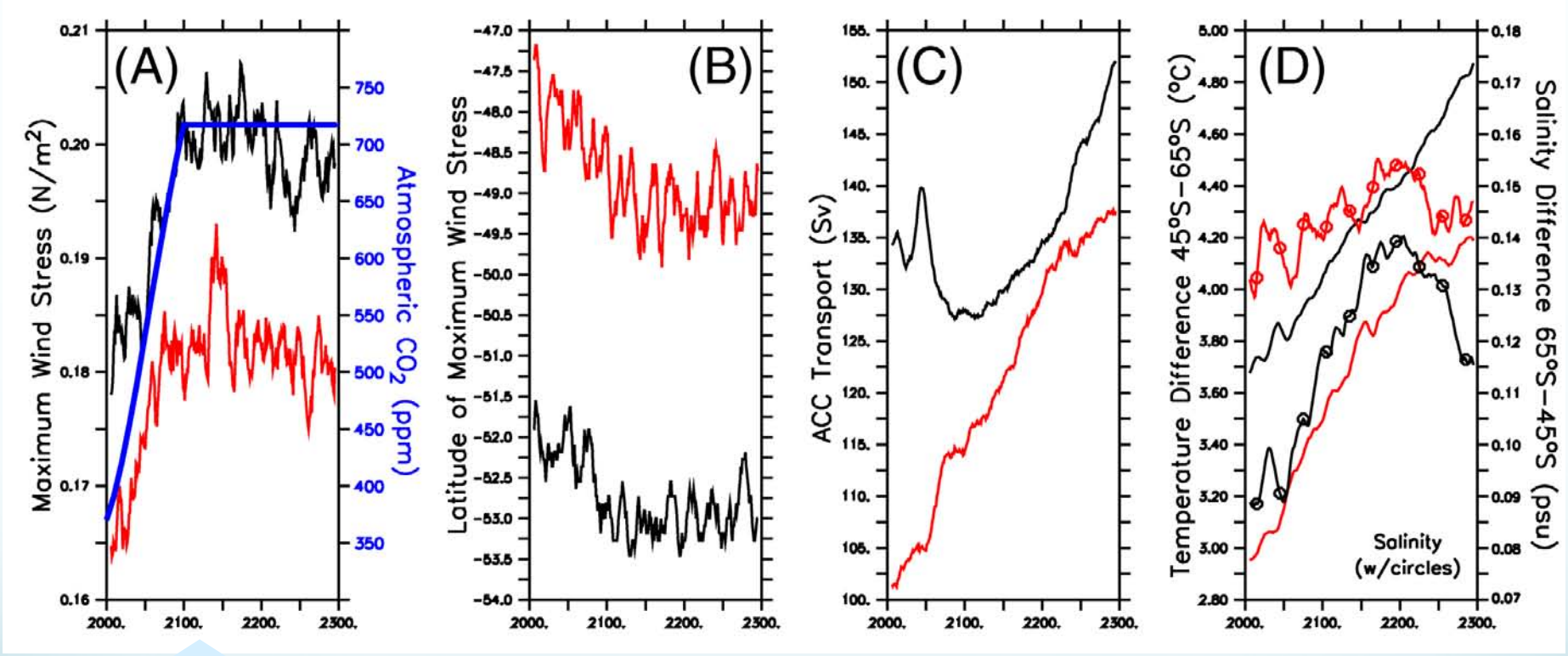

Red=CM2.0, Black=CM2.1

…as CO_2 increases (~doubles), the S. Hemisphere's westerly winds strengthen (max zonal wind stress + ~10%)

Russell et al. (2006a)

Heat and "Carbon" Storage Difference in 2300

CM2.1 - CM2.0 (2300-2000)

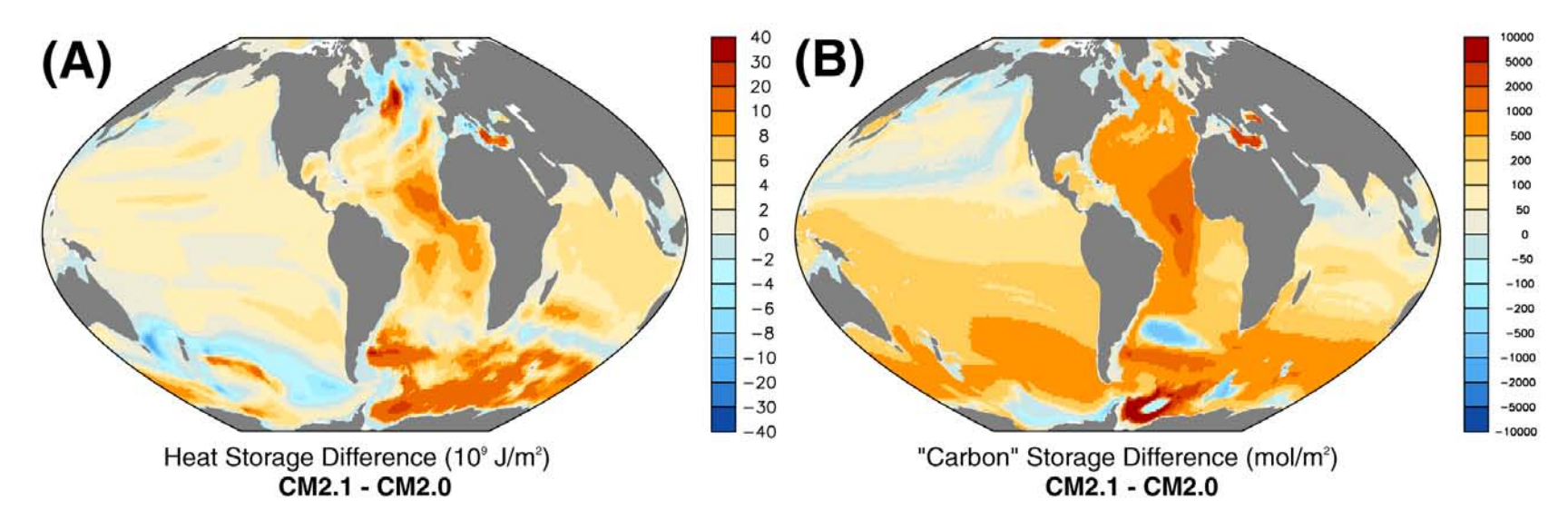

Heat Storage Difference (10^9 J/m^2)

Carbon Storage Difference (mol/m^2)

Russell et al. (2006b)

BUT Isopycnal Tilt = NO Change in ACC Transport!?!

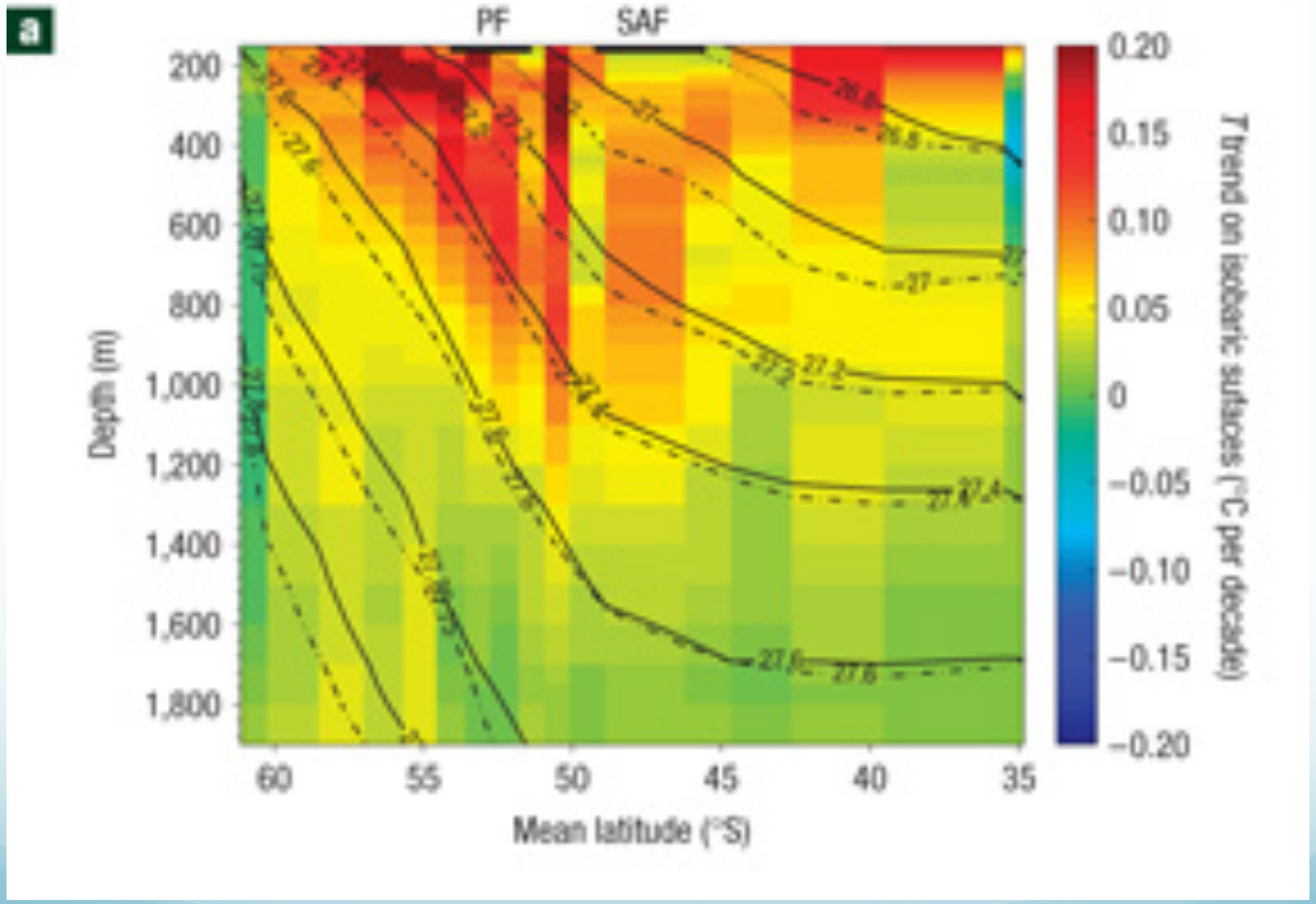

Boning et al., 2008:
From Float data

Depth of AAIW Isopycnal (σ_θ = 27.1)

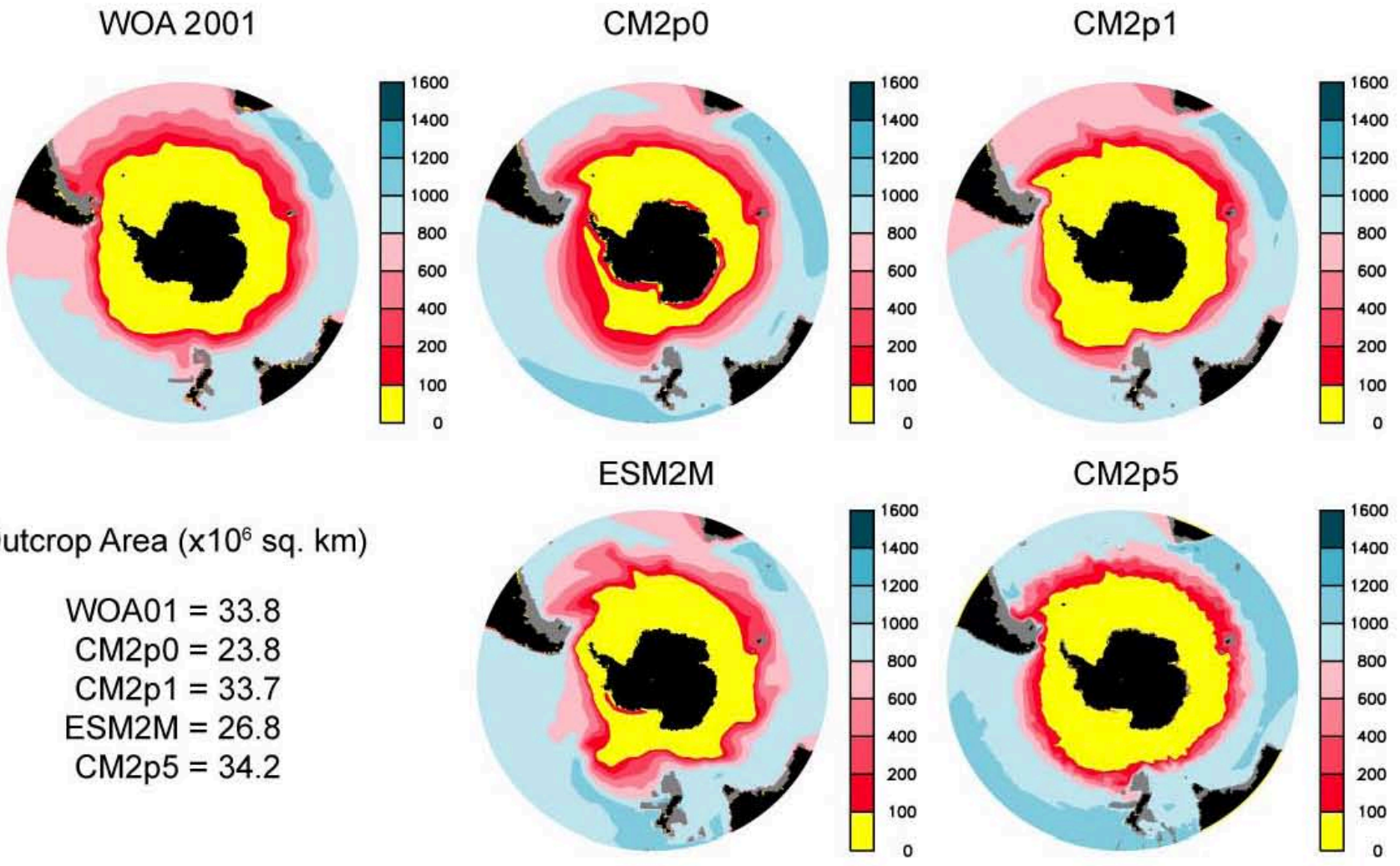

Outcrop Area (x10^6 sq. km)

WOA01 = 33.8
CM2p0 = 23.8
CM2p1 = 33.7
ESM2M = 26.8
CM2p5 = 34.2

Zonal-Mean Potential Vorticity

WOA09

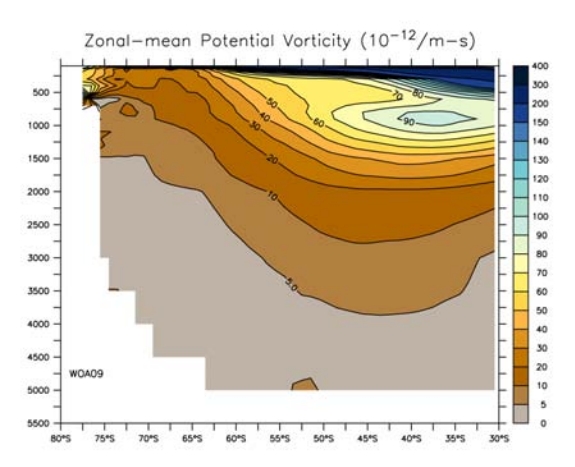

CM2.5

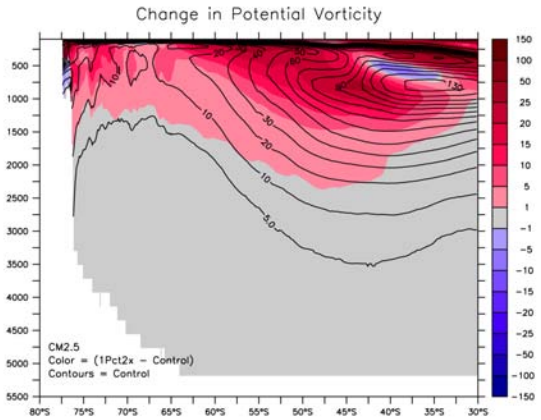

CM2.4

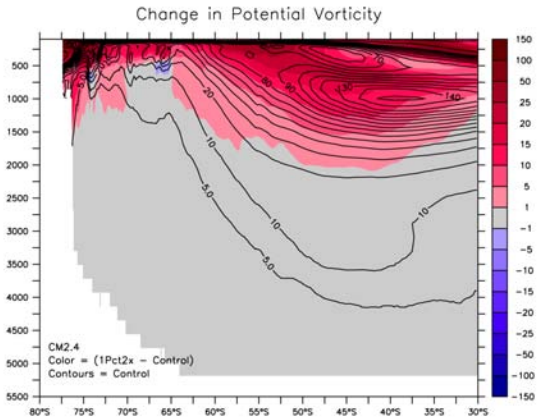

Color = Change in PV
Contour = PV in Control

$$PV = \frac{f}{\sigma_2} \times \frac{\partial \sigma_2}{\partial z}$$

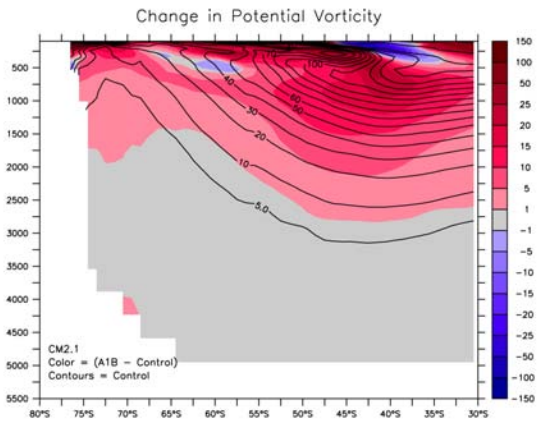

CM2.1

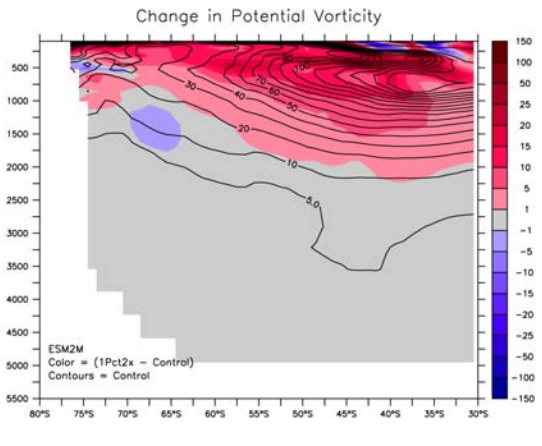

ESM2M

Zonal-Mean Potential Density (σ_2)

WOA09

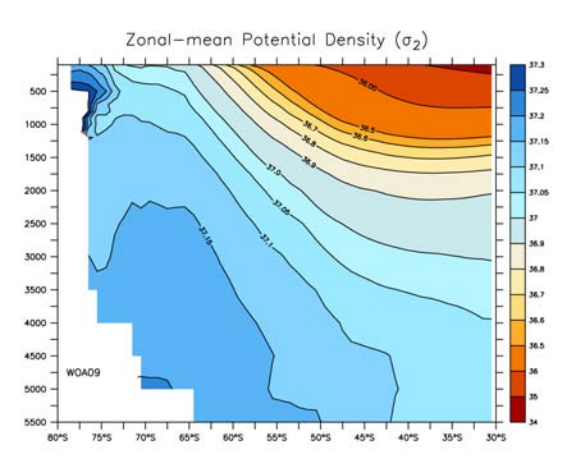

CM2.5

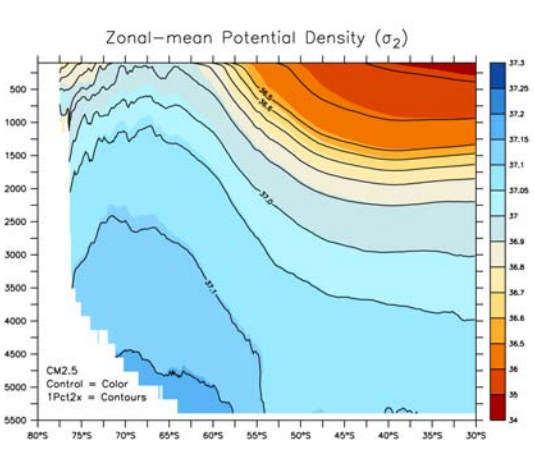

CM2.4

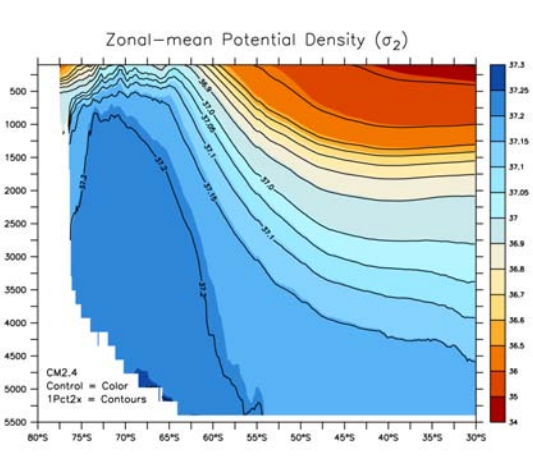

Color = Control
Contour = 1Pct2x

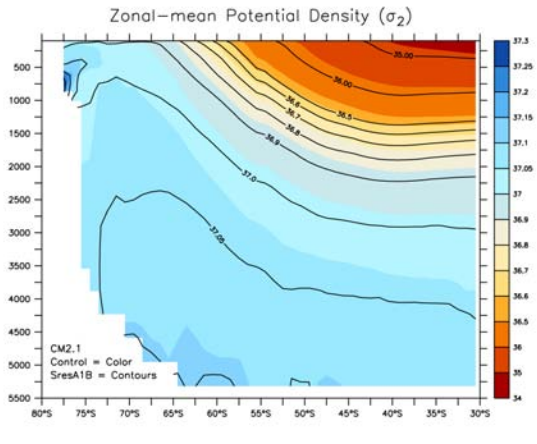

CM2.1

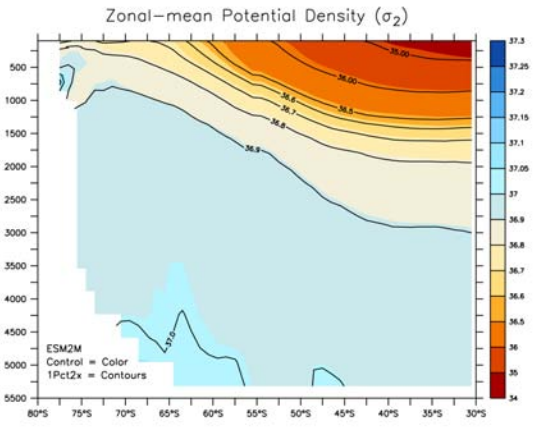

ESM2M

Zonal-Mean Potential Density (σ_2)

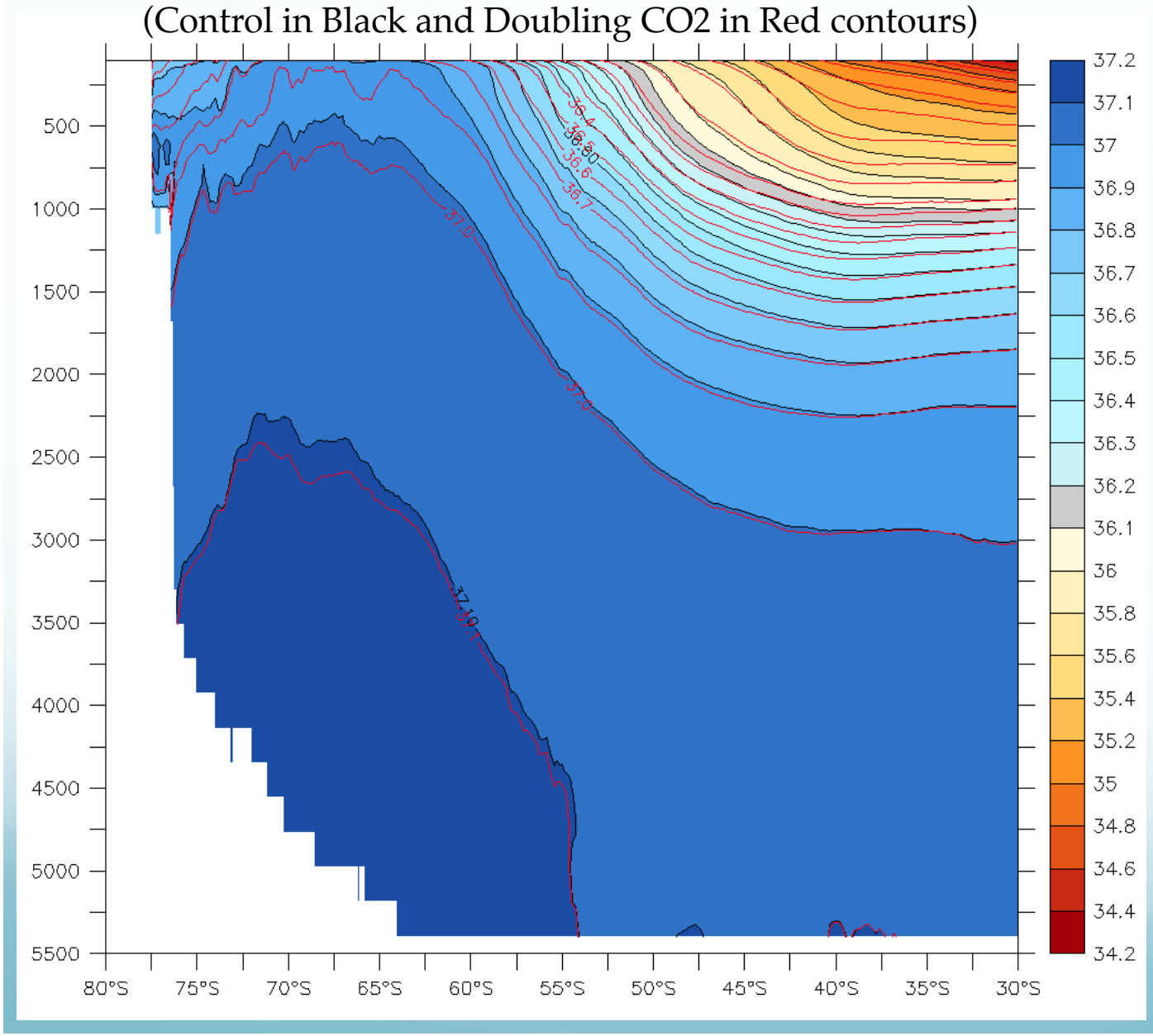

CM2.5

Shallow Warming leads to slumped isopycnals = unchanged ACC

Deep Warming leads to steeper isopycnals = faster ACC

Change in Heat Content

(3000-5500m, 10^9 J/m^2)

CM2.5

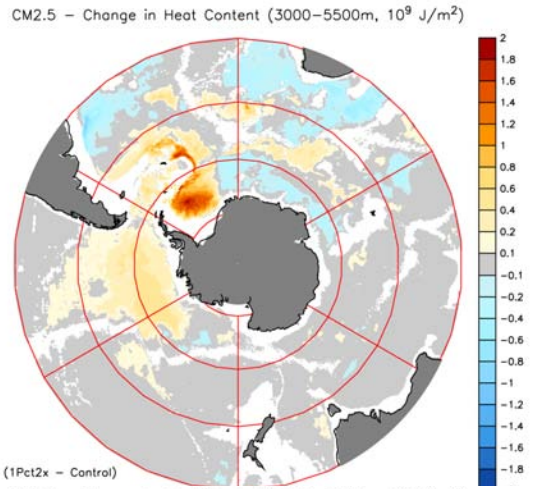

CM2.4

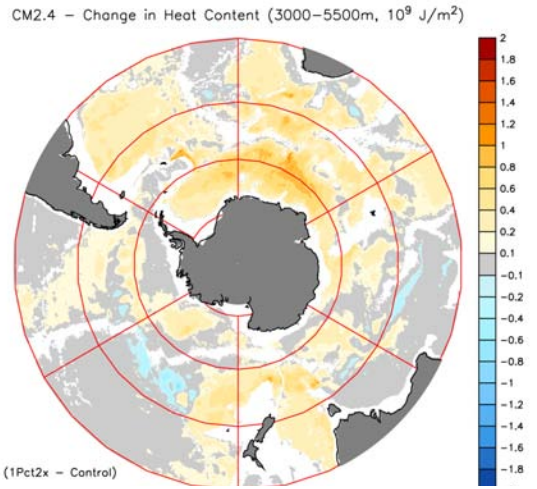

CM2.1

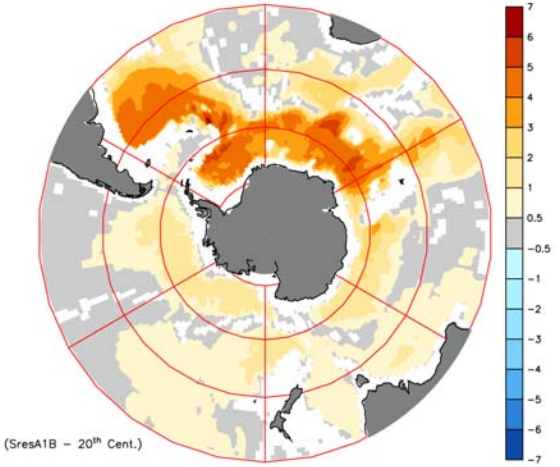

ESM2M